REPUBLIC OF TURKEY
YILDIZ TECHNICAL UNIVERSITY
GRADUATE SCHOOL OF NATURAL AND APPLIED SCIENCES

INVESTIGATION OF CHYMOTRYPSIN-POLY (ACRYLIC ACID) COMPLEX ACTIVITIES BY FLUOROMETRIC METHODS

SAMA AMER

MSc. THESIS
DEPARTMENT OF CHEMISTRY
PROGRAM OF BIOCHEMISTRY

ADVISER
PROF. DR. EMİNE KARAKUŞ

İSTANBUL, 2017

REPUBLIC OF TURKEY
YILDIZ TECHNICAL UNIVERSITY
GRADUATE SCHOOL OF NATURAL AND APPLIED SCIENCES

INVESTIGATION OF CHYMOTRYPSIN-POLY (ACRYLIC ACID) COMPLEX ACTIVITIES BY FLUOROMETRIC METHODS

This study was supported by Yildiz Technical University Scientific Research Projects Coordination Unit, [2012-01-02-KAP10]

ACKNOWLEDGEMENTS

I would like to thank,

My adviser Prof. Dr. Emine KARAKUŞ, who guides and supports me in conducting MSc project, I have benefited greatly from her experiences and knowledge,

Prof. Dr. Barbaros NALBANTOĞLU , for his helping and support I'm really grateful to him,

Dr. İbrahim Ethem ÖZYİĞİT, who helped me in this work. I have benefited from his experience in the laboratory,

All staff of the Department of Chemistry and my colleagues at Yildiz Technical University,

My family, dad, mom, sisters, and brother, who have given me all support and encouragement,

It was impossible without you, I am grateful to you all.

June, 2017

Sama AMER

TABLE OF CONTENTS

Page

LIST OF SYMBOLS

F(t)	Fluorescence intensity
Ia	Absorption intensity
Kd	Distribution coefficient between fixed and moving phases
Mw	Molecular weight
ns	Nanoseconds
PM-BSA	N-(1-Pyrenyl)maleimide- Bovine serum albumin Complex
Qf	Quantum yield
S_0	Ground state
S_1	Excited singlet state
s	Second
T	Triplet state
V_0	The free volume outside the gel particles
V_R	Retention volume
V_g	The volume occupied by the solid matrix of gel
V_i	The volume of solvent held in the pores
V_t	Total column volume
τ	Fluorescence lifetime
α_i	pre-exponential factor

LIST OF ABBREVIATIONS

BSA	Bovine Serum Albumine
Cys	Cysteine amino acid
CF	Correction factor
DMSO	Dimethyl sulphoxide
EDC	1-ethyl-3- (3-dimethylaminopropyl) carbodiimide
ESM	Exponential Series Method
Lys	Lysine amino acid
PAA	Poly (acrylic acid)
PBS	Phosphate buffer solution
PM	N- (1-Pyranyl) maleimide
Tris.HCl	Tris hydrochloride
UV-VIS	Ultraviolet-Visible

LIST OF FIGURES

Page

LIST OF TABLES

Page

ABSTRACT

INVESTIGATION OF CHYMOTRYPSIN-POLY (ACRYLIC ACID) COMPLEX ACTIVITIES BY FLUOROMETRIC METHODS

Sama AMER

Department Of Chemistry

MSc. Thesis

Adviser: Prof. Dr. Emine KARAKUŞ

Conjugation and immobilization of enzymes with polymers have achieved tremendous attention in the last few years. The conjugation of different synthetic polymers onto enzymes has been done to improve catalytic stability of enzymes and can expand the applications of the neutral catalysts. There are many materials, including synthetic organic polymers, biopolymers, hydrogels, inorganic supports, and smart polymers, to be used to immobilize enzyme, and good activity retention, and enhanced thermostability are often observed. There exist a range of functional groups which can be used in the covalent immobilization of enzymes, including amino, hydroxyl, carboxyl and phenolic groups.

In this study, we examined the activity of covalent conjugate of chymotrypsin enzyme with poly (acrylic acid) (PAA) on fluorescence lifetime distributions of the substrate Bovine Serum Albumin (BSA) modified with N-(1-pyrenyl) maleimide (PM) complex. The time resolved spectrofluorometer was used to display the fluorescence decays, which were analysed by using the Exponential Series Method (ESM) to obtain the changes of fluorescence lifetime distributions. After the exposure of the synthesized substrate "PM-BSA" to the bioconjugate "PAA-chymotrypsin", the fluorescence lifetime distributions exhibited different profiles in varying range of lifetime scales, indicating a significant decrease in the activity, relatively to the one of free chymotrypsin. This study may have a guiding importance for the determination of the most appropriate conjugation method and choosing the right polymer, to improve the stability of chymotrypsin-like proteases without losing the activity in bioconjugation researches.

Keywords: Conjugation, poly (acrylic acid) (PAA), chymotrypsin, fluorescence lifetime distributions, Bovine Serum Albumin (BSA), N-(1-pyrenyl)maleimide, Exponential Series Method (ESM)

ÖZET

KİMYOTRİPSİN-POLY (AKRİLİK ASİT) KOMPLEKSİ AKTİVİTELERİNİN FLOROMETRİK YÖNTEMLER İLE İNCELENMESİ

Sama AMER

Kimya Anabilim Dalı

Yüksek Lisans Tezi

Tez Danışmanı: Prof. Dr. Emine KARAKUŞ

Polimerlerle enzimlerin konjugasyonu ve immobilizasyonu son birkaç yıldır büyük ilgi görmüştür. Farklı sentetik polimerlerin enzimlerle konjugasyonu, enzimlerin katalitik stabilitesini arttırmak için yapılmıştır ve nötral katalizörlerin kullanımını genişletebilir. Enzimleri hareketsiz kılmak üzere kullanılacak sentetik organik polimerler, biyopolimerler, hidrojeller, inorganik destekler ve akıllı polimerler de dahil olmak üzere pek çok malzeme vardır ve iyi aktivite tutma ve gelişmiş termostabilite sıklıkla gözlenir. Enzimlerin kovalent immobilizasyonunda kullanılabilen amino, hidroksil, karboksil ve fenolik grupları içeren bir dizi fonksiyonel grup bulunmaktadır.

Bu çalışmada, N-(1-pirenil) maleimid (PM) kompleksi ile modifiye edilmiş sığır Serum Albümin (BSA) substratının floresans ömür dağılımları üzerinde, kimotripsin enziminin poli (akrilik asit) (PAA) ile kovalent konjugatının aktivitesini inceledik. Zaman ayrımlı spektroflorometre, floresans ömür dağılımlarını elde etmek için Üstel Seriler Metodu (Exponential Series Method; ESM) kullanılarak analiz edilen floresans bozunmalarını görüntülemek için kullanıldı. Sentezlenen substrat "PM-BSA"nın biyokonjugat "PAA-kimotripsin"e maruziyeti sonrası, floresan ömür dağılımları, serbest kimotripsine maruziyetine görece aktivitede önemli bir düşüş olduğunu anlatan, ömür ölçeklerinin farklı aralıklarında farklı profiller sergiledi. Bu çalışma, biyokonjüjasyon araştırmalarında aktiviteyi kaybetmeden, kimotripsin benzeri proteazların stabilitesini arttırmak için en uygun konjugasyon yönteminin belirlenmesi ve doğru polimer seçimi için yol gösterici bir öneme sahip olabilir.

Anahtar kelimeler: Konjugasyon, poli (akrilik asit) (PAA), kimotripsin, floresans ömür dağılımları, sığır serum albümin (BSA), N-(1-pirenil)maleimid, üstel seriler yöntemi (Exponential Series Method; ESM)

CHAPTER 1

INTRODUCTION

1.1 Literature Review

The marking of biologically active molecules and their use, especially for quantitative or qualitative determination, goes back to 1950. The preparation of immunological kits by marking and using antigens or antibodies using radioactive material was carried out in 1960 and after. In the following years, the use of enzymes and fluorescent substance-labeled biological molecules, and the development of kits for use in clinical specimens, have gained considerable speed and have been used for labeling various fluorescent substances. Taking of long-lived fluorescent substances place in the biomarking processes and the development of time-resolved fluorometers, has allowed the preparation of highly sensitive clinical kits. Fluorescence spectroscopy is especially used for the investigation of structural states of biomolecules and for the purpose of tracking of many reactions. The time-resolved fluorescence technique, which has been widely used in recent years, allows the decay profiles of emission and time-resolved spectra. Thus fluorescence lifetimes can be calculated and intermolecular interactions, solvent effects can be monitored [1-6].

The determination of enzyme activity on the substrates by fluorometric methods is carried out by evaluating the photophysical data obtained from the changes of fluorescence properties of intrinsic or extrinsic fluorescent molecular groups which take place in the substrate structure. Fluorometric data can be obtained from the parameters; the maximum emission wavelength shift in the emission spectra, decreasing or increasing of emission intensity, quenching of emission, the variation of fluorescence decay profiles by means of time, the changing and variation of fluorescence lifetimes [1-6].

Proteolytic enzymes and their inhibitors play a fundamental and vital role in the metabolism activities of living organisms such as cell cycle control, growth and differentiation, gene expression, enzyme modification, immunological reactions, tissue formation, apoptosis [7, 8, 9].

Pyrene derivatives are used as fluorescent adducts in the determination of functional group amount of biomolecules [1], membrane permeability [2,10,11], kinetic parameters of enzymes [12], tracking the conformational changes [13,14], and interactions between subunits [15]. The pyrene maleimide derivative is used as a fluorescent label in specific labeling of free sulfhydryl (-SH) groups under the reaction conditions near neutral pH [1]. The very little changes in enzyme-induced substrate dynamics can be detected sensitively by fluorescence measurement methods, even if the other organic substances and salts have been at high concentrations in the medium. Bioconjugation defines the linking of two biomolecules, for example protein–protein, carbohydrate–protein, polymer–protein conjugates and also involves the attachment of synthetic labels (isotope labels, fluorescent dyes, affinity tags, biotin) to biomolecules such as carbohydrates, proteins, peptides, synthetic polymers, enzymes, glycans, antibodies, nucleic acids, and oligonucleotides [16]. Protein–polymer conjugates are biohybrid materials and can combine the advantages of both components and avoid the disadvantages of each separate component. For example, proteins may acquire a higher chemical and thermal stability in their conjugated forms with polymers. In spite of all the benefits of the conjugation, a wrong linking can reduce or inactivate the protein bioactivity, by covering the binding sites or catalytic centers or using necessary amino acid residues for the linkage. In the view of this point it is important to selection of the most suitable polymer and the right conjugation method [17, 18].

1.2 Objective of the Thesis

The aim of this work is to compare the differences between the proteolytic effects of free and bioconjugate form of the digestive enzyme chymotrypsin with high-molecular weight poly acrylic acid (PAA) [(PAA-chymotrypsin)], on the substrate bovine serum albumin (BSA) modified with N-(1-pyrenyl) maleimide [(PM-BSA)], by tracking the changes in fluorescence lifetime distributions.

1.3 Hypothesis

Conjugation of biomolecules with polymers forms a new chemical environment around the biomolecules. The new structure may make them more stable against to the destructive effects of solvent cage and enzymatic degradation. This information caused new wide researches on the conjugates of biomolecules.

Fluorescence lifetime distributions may be useful tool to monitor the changes of enzyme activity by the conjugation with polymers. Fluorophores which are embedded in different regions of proteins have different chemical environments and exhibit varying fluorescence lifetimes that produce a specific fluorescence lifetime distribution profile. The changes of the distribution by the proteolytic enzyme (protease) activity provides useful information about the hydrolysis process of the protein substrate. The hydrolysis makes fluorophores exposure to the solvent more and the lifetime distribution shifts to the shorter region. By using this mechanism, the differences between the proteolytic activities of free chymotrypsin and the bioconjugate "PAA-chymotrypsin" may be monitored by the differences between the lifetime distributions of the proteolytic hydrolysates of PM-BSA produced by the two forms of chymotrypsin, if the two hydrolysates have remarkable different peptide content from each other, which make different chemical environments around the fluorophores causing the fluorescence lifetime variations.

CHAPTER 2

GENERAL INFORMATION

2.1 Structural Units of Enzymes

Enzymes are biocatalysts, which are actually proteins. For this reason, in order to understand the structure and function of enzymes, it is necessary to examine the protein structure and the amino acid constituting the protein structure and combine the amino acid units with each other by special binding.

2.1.1 THE α-Amino Acids

Amino acids, are molecules containing **amino** (-NH2) and **carboxylic acid** (-COOH) groups linked to the center alpha carbon (Cα), and this alpha carbon also linked to (R) group (Figure 2.1) [19].

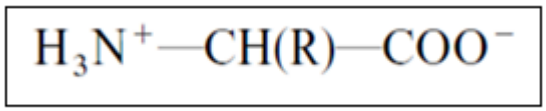

Figure 2.1 The general structure of amino acids [19]

There are usually 300 amino acids in nature, but only 20 amino acids are present in proteins structure. Almost, all amino acids can be found in two forms, D and L-α-amino acids forms, except glycine which has –H group as (R) group. These amino acids found in the structure of proteins are named L-α-amino acids. The structures of the twenty natural L-α-amino acids, sorted by the polarity of the (R) groups. The abbreviations three-letter and one-letter used for each amino acid to represent the amino acids in peptides [20].

Table 2.1 The 20 L-α-amino acids in proteins [20]

Name	Symbol	Structural Formula	pK_1 α-COOH	pK_2 α-NH_3^+	pK_3 R Group
With Aliphatic Side Chains					
Glycine	Gly [G]	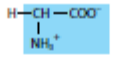	2.4	9.8	
Alanine	Ala [A]	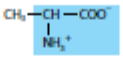	2.4	9.9	
Valine	Val [V]	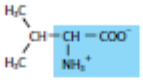	2.2	9.7	
Leucine	Leu [L]	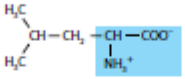	2.3	9.7	
Isoleucine	Ile [I]	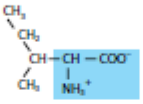	2.3	9.8	
With Side Chains Containing Hydroxylic (OH) Groups					
Serine	Ser [S]	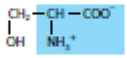	2.2	9.2	about 13
Threonine	Thr [T]	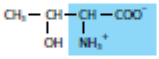	2.1	9.1	about 13
Tyrosine	Tyr [Y]	See below.			
With Side Chains Containing Sulfur Atoms					
Cysteine	Cys [C]	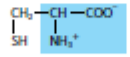	1.9	10.8	8.3
Methionine	Met [M]	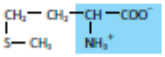	2.1	9.3	
With Side Chains Containing Acidic Groups or Their Amides					
Aspartic acid	Asp [D]	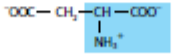	2.0	9.9	3.9
Asparagine	Asn [N]	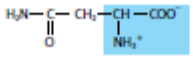	2.1	8.8	
Glutamic acid	Glu [E]	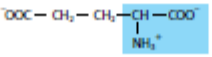	2.1	9.5	4.1
Glutamine	Gln [Q]	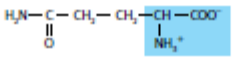	2.2	9.1	

With Side Chains Containing Basic Groups			α-COOH	α-NH_3^+	R Group
Arginine	Arg [R]	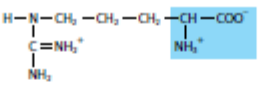	1.8	9.0	12.5
Lysine	Lys [K]	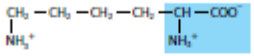	2.2	9.2	10.8
Histidine	His [H]	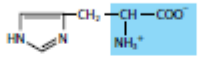	1.8	9.3	6.0
Containing Aromatic Rings					
Histidine	His [H]	See above.			
Phenylalanine	Phe [F]	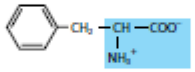	2.2	9.2	
Tyrosine	Tyr [Y]	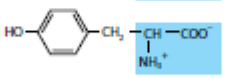	2.2	9.1	10.1
Tryptophan	Trp [W]	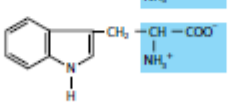	2.4	9.4	
Imino Acid					
Proline	Pro [P]	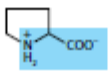	2.0	10.6	

The L-α-amino acids are linked together by condensation reaction between α-carboxyl group of one amino acid and α-amino group of the other amino acid through the formation of peptide bonds with releasing of water molecule to form a dipeptide (Figure 2.2) [21].

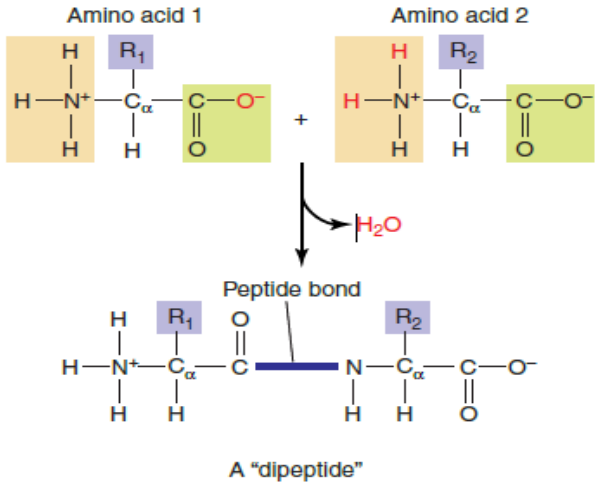

Figure 2.2 Two amino acids linked by peptide bond [21]

X-ray crystallography studies on small peptides exposed that CN and CO structures within the peptide have a bond length between the single bond (CN, CO) and double bond (C = N, C = O) The length of the peptide bond is 60% C = O and 40% C = N (Table 2.2) [19].

Table 2.2 Typical bond lengths for carbon-oxgen and carbon-nitrogen bonds [19]

Bond Type	Bond Length (Å)
C—O	1.27
C═O	1.22
C—N	1.45
C═N	1.25

The stability of the 40% double bond character formed along the C-N axis to the peptide bond inhibits the rotation around the peptide bond. Therefore, the six atoms in the peptide unit form a planar array of planes, bringing the plane of the peptide to the center. This planar structure limits the number of spatial configurations that the peptide can adapt itself. In the peptide plane, carbon stereochemistry may be formed by

carbonyl oxygen and nitrogen protonation at the opposite side of the axis defined by the C-N bond.

Two stereoisomers of the peptide planer can be formed depending on the location of the carbonyl oxygen and nitrogenous proton: **cis** stereoisomer, when these groups settlement on the same sides of the C-N bond, **trans** stereoisomer may occur when these groups settlement on opposite sides of the C-N bond. However, the steric hindrance of the side chains of amino acids in the cis stereoisomer structure make all the natural peptides are synthesized in the trans stereoisomer structure since it is more convenient than cis (Figure 2.3)

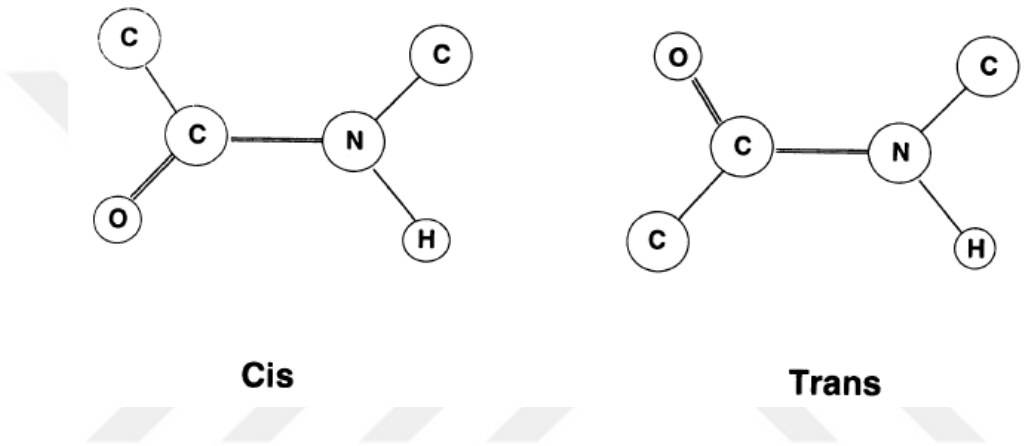

Figure 2.3 cis and trans configurations of the peptide bond [19]

Proteins differ from each other in properties; the sequence of amino acids in the polypeptide chain, total number of amino acids in the protein structure and the complexes they make with non-protein molecules such as carbohydrates and lipids [19].

2.1.2 Structural Properties of Proteins

Proteins; They exhibit four different structural types : primary , secondary , tertiary and quaternary

2.1.2.1 Primary Protein Structure

The structure and reactivity of a protein are defined by the identity of the amino acids that make up its polypeptide chain, and according to the order of the amino acids in the chain. the primary structure is defined by the sequence in which the amino acids form the polymer. By convention, the sequence is written as follows, beginning with the N-terminus on the left (Figure 2.4) Almost all intracellular proteins of the primary structures consist of linear polypeptide chains [22].

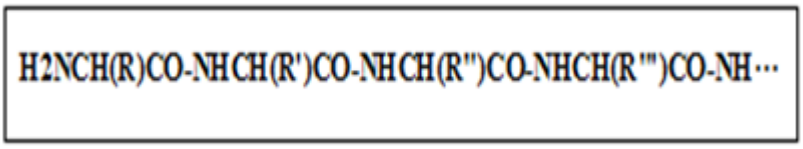

Figure 2.4 Primary protein structure [22]

The order of the amino acids sequences in the polypeptide chain is determined according to the genetic codes of the DNA structure. Any change in these genetic codes may lead to a change in the sequence of amino acid in the protein. Even if the change in one amino acid in a protein sequence can affect on the structure and function of protein [19].

2.1.2.2 Secondary Protein Structure

Proteins exhibit two types of secondary structure, the right handed "α-helix" and β-pleated sheet. Both of these structures have an significant role of the total conformation of any protein .

2.1.2.2.1 The Right Hand "α-Helix"

In the Right Hand "α-Helix" the hydrogen bonds between the oxygen of the (C=O) and hydrogen of the (N-H) groups extending between the folds ensure the stability of the structure. The polypeptide chain is folded about an axis in the direction of the right hand grip. Each cycle of the helix structure contains 3.6 amino acids and the distance between the folds is about 0.54 nm. The vertical rise per residue is 0.15 nm/residue (0.54nm/3.6 residues) [19].

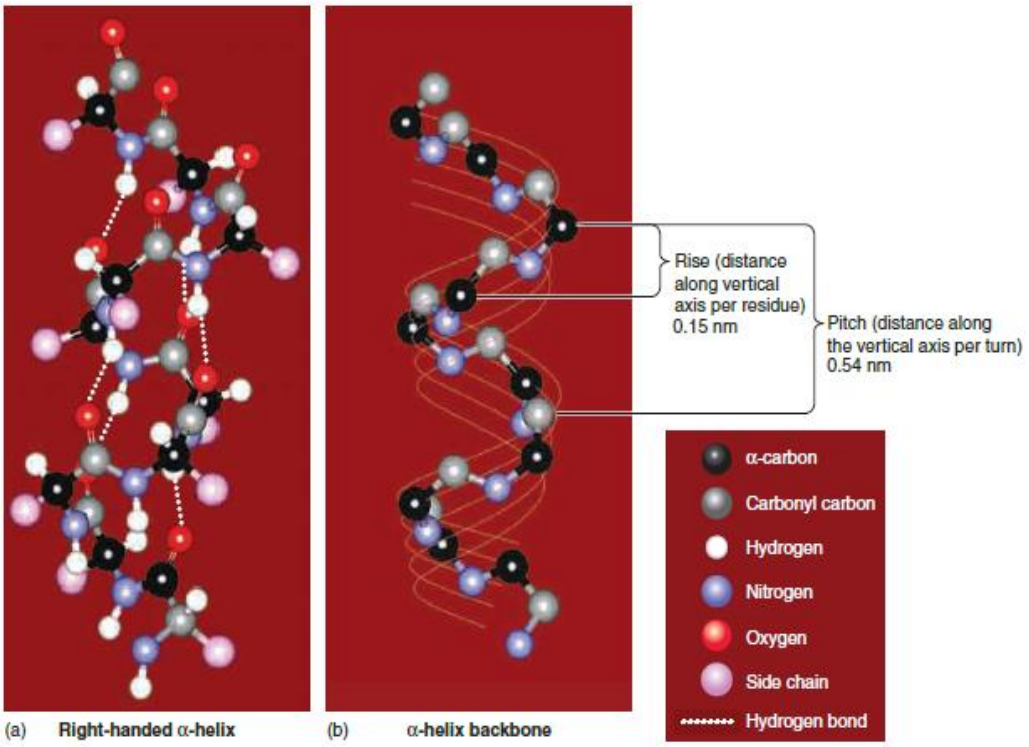

Figure 2.5 **(a)** Right-hand "α-helix" **(b)** Backbone of α-helix [21]

2.1.2.2.2 The β -Pleated Sheet

Two or more segments of a polypeptide chain in parallel side by side, resulting in hydrogen bridge bonds formed between the -NH and -CO groups, forming a β-pleated sheet structures. The hydrogen bonds formed between the -NH and -CO groups of these adjacent chains increase the structural stability [19]. The β-pleated sheet structure may be parallel, if the polypeptide chains can line up side by side so that -NH and –CO groups on adjacent chains extend in the same direction (Figure 2.6-A), or anti-parallel, if present on the opposite direction (Figure 2.6-B)[21].

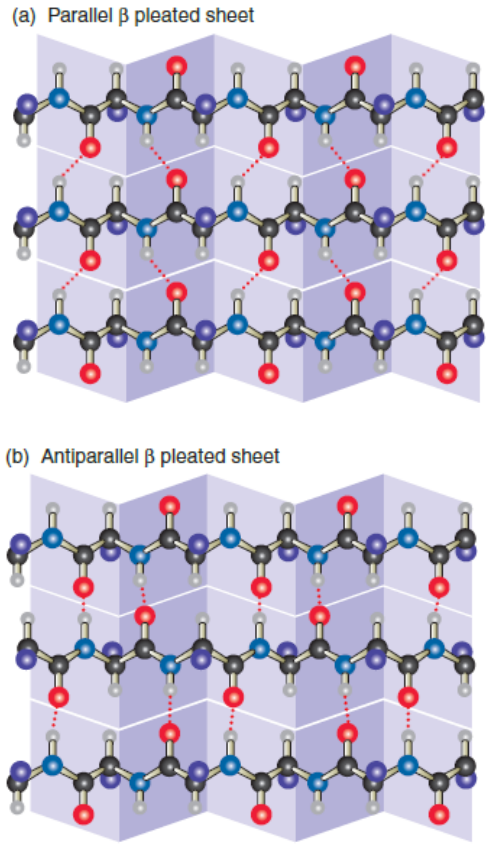

Figure 2.6 β-folded layers structures [21]

2.1.2.3 Tertiary Protein Structure

The secondary structural of protein (α-Helix and β-Pleated Sheet) arrange in three dimensional conformation, this lead to interact amino acid side chains and connected with each other to eventually form a folded protein it is referred to as the tertiary protein structure (Figure 2.7). The van der Waals forces, hydrophobic bonds, ionic bonds and disulfide bonds, all these forces have specific binding affinities to the polypeptide chains and give more stability for the three dimensional structure of protein. The tertiary structure of each protein is unique; this feature allows proteins to be specialized in certain tasks in the organism [19].

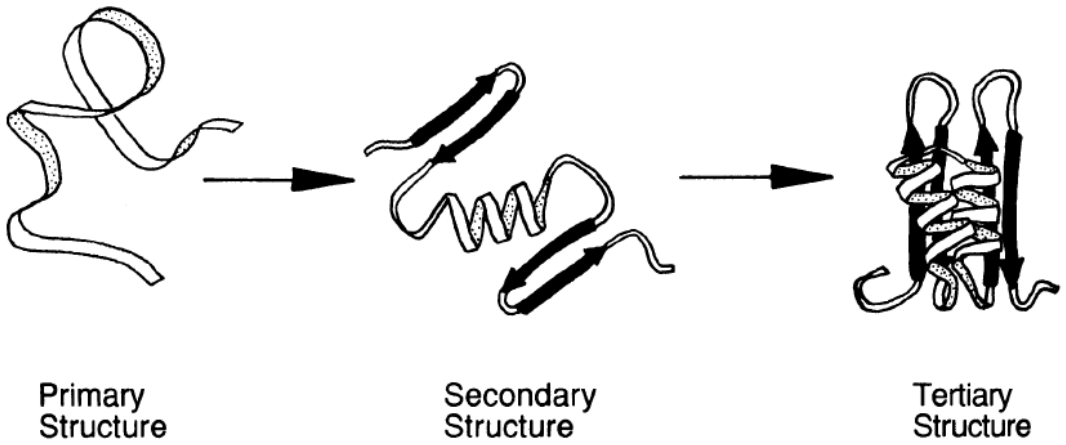

Figure 2.7 The folding of a polypeptide chain into a tertiary structure [19]

2.1.2.4 Quaternary Protein Structure

In many cases in order to get an effective protein that requires more than one folded polypeptide chain. Quaternary protein structures; Are structures made up of more than one folded of polypeptide chains come together with covalent bonds, ionic bonds, van der Waals forces and hydrophobic interactions. Each single polypeptide in the quaternary structure is called subunit. When the subunits separate from each other, protein function is lost. Non covalent forces between the subunits help to stabilize the overall structure, such as hydrogen bonding, salt bridge formation, and hydrophobic interactions. An example of a protein quaternary structure: Hemoglobin; carries oxygen from the lungs to the muscles [19].

The four levels of protein structure are illustrated in (Figure 2.8).

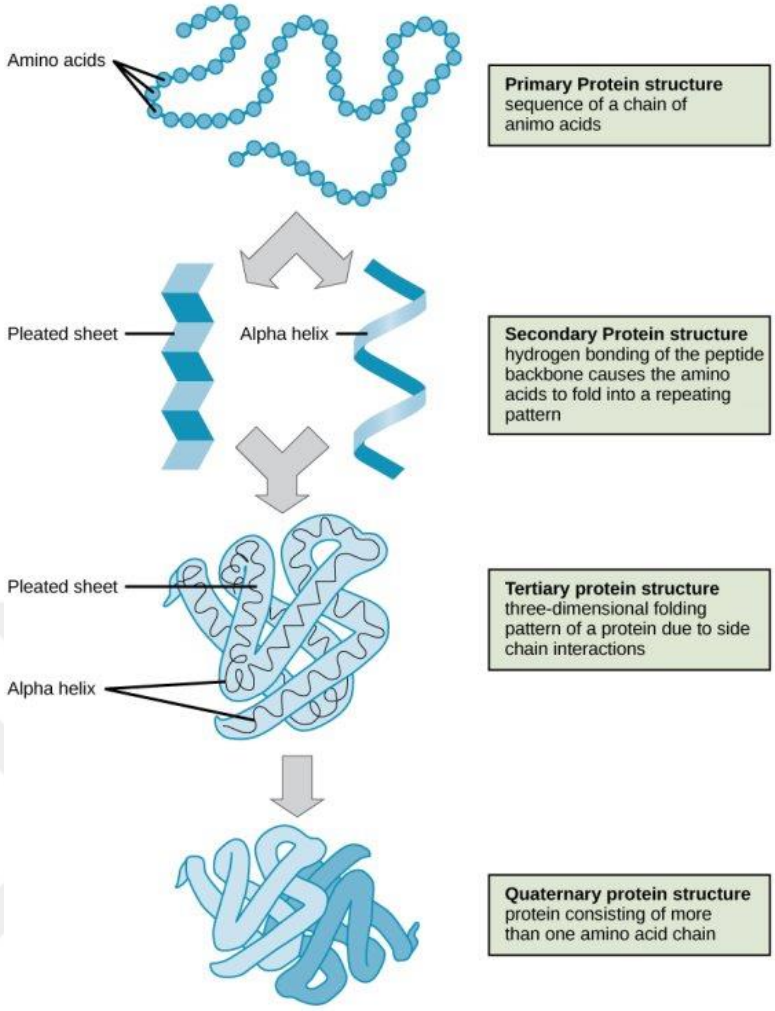

Figure 2.8 The four levels of protein structure [23]

2.2 Structure and Catalysis of Enzymes

Enzymr wich are the three-dimensional structures are the cornerstone for stimulating biochemical reactions. The substances that the enzymes act as catalysts are called (substrates). The part of the enzyme where the substrate binds is called the active site. in order to understand the rate of increase in enzymatic reactions, it is necessary to examine the structure of this active site and its reaction with the substrate. However, the three-dimensional nature of the enzyme as a whole is also influenced by its catalytic activity and substrate specificity. Enzymes are very specific catalysts that are selective for both reaction types and substrates due to the specific design of active site. The selectivity for the substrates of the enzymes is concerning with the structure of the active site. The geometry of the active site, mostly in the form of an asymmetric cavity, is compatible with the three-dimensional structure of the substrate, facilitating entry into this region [19].

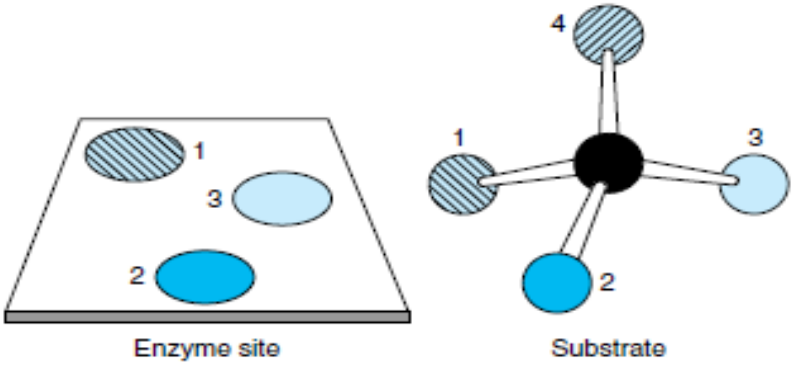

Figure 2.9 Planar representation of the "three-terminal" of a substrate to the active site of an Enzyme. atoms 1 and 4 are identical, once atoms 2 and 3 are bound to their complementary sites on the enzyme, only atom 1 can bind. Thus enzyme binding allows identical atoms to be distinguished stereospecifically from each other [20]

Understanding the bonding and catalysis mechanism of the enzyme and substrate intrigued scientists for a long time. In 1894, Emil Fischer developed the first Model to explain enzyme function called the key-lock model; this model introduces the principle of Three-dimensional complementarity. A substrate binds to the active site of enzyme just like a key fits into a lock, and the converging enzyme-substrate pair forms the ES complex. This model is greatly simplified, where it does not explain what happens to enzyme after it binds to the substrate .Then, in 1930, J.B.S. Haldane concluded that the active site of enzyme has mor affinity to the transition state , that lead to increased stability and catalytic force of enzyme. In 1960, Koshland suggested an idea modified to Helen model. In this model (Koshland/ Haldane model), the activity of enzyme increases after enzyme binding with ground state. This main idea is improvement in that it realized that the chemical power of the both substrate and enzyme must effect to one another in the process of binding. Although these models have some approaches to enzyme specificity, they do not give a clear idea of how the catalytic reaction rate will increase. The quantitative enzymatic reaction studies have shown that the increase of catlytic rate is due to the specific binding of the active site which is increasing the stability of the ES complex and the proximity of the molecules to each othe. In 1993, Billy Mark Britt proposed a new model with the name Shifting Specificity Model (SSM) (Figure 2.10) . According to this model; The native enzyme (the folded form at its physiological pressure, temperature, and PH) forms the ES complex through weak bonds established by the substructure in the unchanged active site which fully conforms to the substrate as in Fischer's key-lock model. This binding triggers a twisting motion

that leads to a three dimensional structure of the entire enzyme mass. While the shape of the active side changes only with this torsional motion, the specificity of the substratum in the basic state is also adapted to the conformational changeover transition [24].

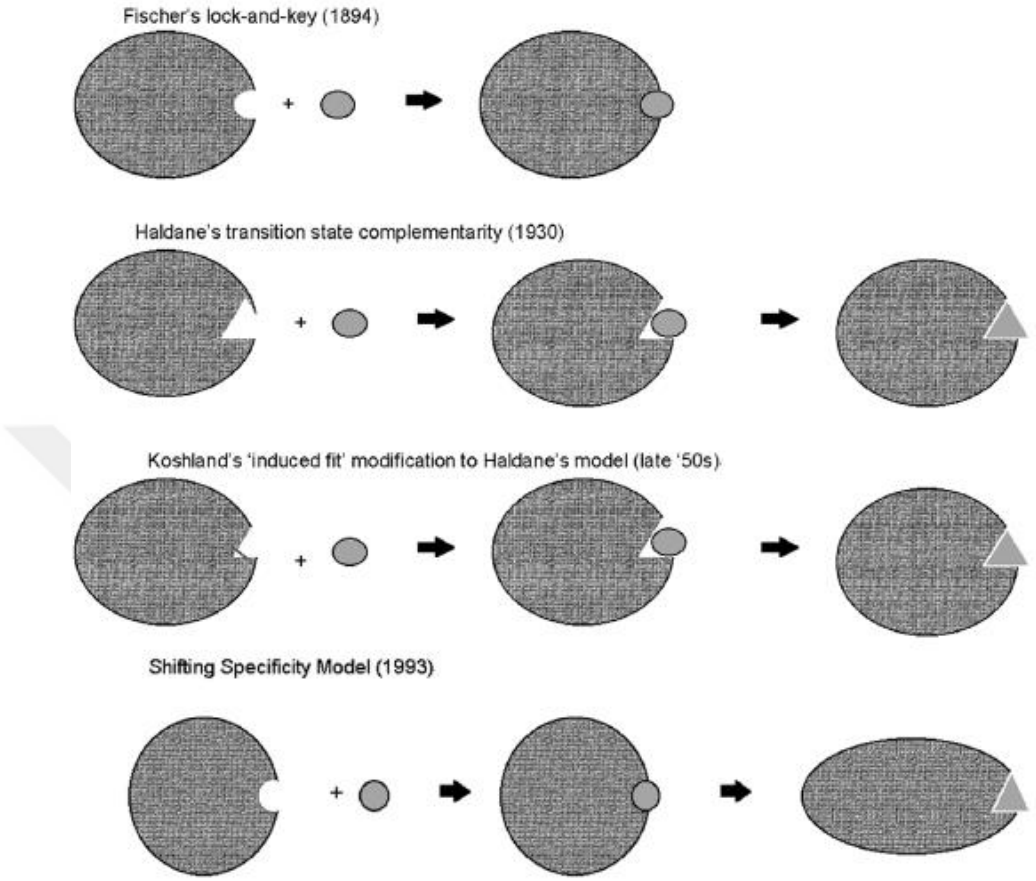

Figure 2.10 Enzyme catalysis models [24]

Some enzymes may act as catalysts on their own, but some require ancillary substances that are not in the protein structure for catalytic activity and are called **cofactors**. There are two groups of cofactors : Metal Ions as Mg^{2+}, Fe^{2+}, Mn^{2+}, Zn^{2+} and so on , or small organic molecules called **Coenzyme** (Table 2.3). The enzyme is called **apoenzyme** when removal its cofactor ; and called **holoenzyme** when it bind with the cofactor.

(Apoenzyme + cofactor = holoenzyme)

Both (cofactors , coenzyme) are important components to increase the effectiveness and stability of the enzyme [25].

Table 2.3 Types of enzyme cofactors[25]

Cofactor	Enzyme
Coenzyme	
Thiamine pyrophosphate	Pyruvate dehydrogenase
Flavin adenine nucleotide	Monoamine oxidase
Nicotinamide adenine dinucleotide	Lactate dehydrogenase
Pyridoxal phosphate	Glycogen phosphorylase
Coenzyme A (CoA)	Acetyl CoA carboxylase
Biotin	Pyruvate carboxylase
5′-Deoxyadenosyl cobalamin	Methylmalonyl mutase
Tetrahydrofolate	Thymidylate synthase
Metal	
Zn^{2+}	Carbonic anhydrase
Zn^{2+}	Carboxypeptidase
Mg^{2+}	*Eco*RV
Mg^{2+}	Hexokinase
Ni^{2+}	Urease
Mo	Nitrate reductase
Se	Glutathione peroxidase
Mn^{2+}	Superoxide dismutase
K^{+}	Propionyl CoA carboxylase

2.3 Naming of Enzymes

The names of enzymes indicate the chemical reaction catalyzed or the substrate interacted with the enzyme, with names ending in (ase). For example; Dehydrogenase, phosphorylase (enzyme that adds phosphorus), phosphatase (enzyme that hydrolyzes phosphate bond), peptidase, glycosidase, lactase, lipase. There are some enzymes that have specific names; like trypsin, pepsin, and chymotrypsin [25].

2.4 Classification of Enzymes

Enzymes are usullay classified into six groups according to the standards of Enzyme Commission (E.C.), affiliated to the IUPAC-IUBMB (International Union of Biochemistry and Molecular Biology) Joint Committee. These groups were subclasses

and further subclasses, so each enzyme is determined by four numbers preceded by the abbreviation (EC) for Enzyme Commission .

this six groups have been named and numbered, according to the reaction they stimulate [26].

2.4.1 Oxidoreductases

Catalyzes the electronic transfer of the H and O between substrate .

Examples:

(a) EC 1.1.1.27 - lactate dehydrogenase

(b) EC 1.4.1.9 leucine dehydrogenase (reductive amination)

2.4.2 Transferases

catalyzes transfer of particular groups as seen in the general reaction equation below

$$AX + B \overset{\text{X-Transferaz}}{\rightleftharpoons} BX + A$$

X: the group transferred; Enzyme name: X-transferase

Examples:

(a) EC 2.1.1.20 glycine-N-methyltransferase

(b) EC 2.6.1.x transaminase

2.4.3 Hydrolases

Catalyzes hydrolysis of varios kinds of compounds .

Examples:

(a) EC 3.1.1.x lipase

(b) EC 3.5.5.1 nitrilase

2.4.4 Lyases

catalyzes the double bond formation by removing groups from their substrates ; these are a kind of elimination mechanism but are non oxidative or hydrolytic . The converse

reaction stimulates the reaction of the addition, where a group is added to the double bond

Examples:

(a) EC 4.3.1.1 aspartate ammonia lyase (aspartase)

(b) EC 4.1.1.12 L-Asp-β-decarboxylase

2.4.5 Isomerases

Catalyzes isomerization reactions, including rearrange atoms within molecules.

Examples:

(a) EC 5.3.1.1 triose phosphate isomerase

(b) EC 5.1.1.1 alanine racemase

2.4.6 Ligases

catalyzes linking of two substrates with ATP hydrolysis .

Example:

EC 6.2.1.1 Acetyl—CoA synthetase

EC 6.5.1.1 DNA ligase (ATP-dependent) [26 , 27].

2.5 Proteases (E.C.3.4)

Proteolytic enzymes play a main role in the regulation many kinds of physiological and pathological events in living machine are known in the scientific literature as proteases, proteinases, peptidases. These enzymes catalyze the hydrolysis reactions of peptide bonds in peptides and proteins. The term "protease", in the second half of the century, German physiological chemistry was used to indicate proteolytic enzymes in the literature. In order to differentiate the different protease activities that were noticed during and after 1930's; these enzymes have been named by classifying them according to the characteristics of their work .

Peptidases in the EC list contain 13 sub-subclass (Table 2.4). The sub-subclass are split up into two principal types : **exopeptidases** (3.4.11-19) , showing their effectiveness in regions near the end of the polypeptides chains . Those attack at amino(N)-terminus

release a single amino acid (aminopeptidases, 3.4.11), or a dipeptide or a tripeptide (dipeptidyl-peptidases and tripeptidyl-peptidases, 3.4.14) from the peptide chain .The exopeptidases attack at carboxy(C)-terminus release a single residue (carboxypeptidases, 3.4.16-18) or a dipeptide (peptidyl-dipeptidases, 3.4.15). and **endopeptidases** (3.4.21-24 with 3.4.99) , stimulates the split of internal peptide bonds in the polypeptides chains. Those are split up into sub-subclasses according to their catalytic mechanisms in the EC list and their specificity is only used to identify specific enzymes in the group. Serine endopeptidases (E.C.3.4.21) contain a serine amino acid that functions in the catalytic process in its active centers. Likewise, there is a cysteine amino acid in the active centers of the cysteine endopeptidases (E.C.3.4.22), and an aspartic acid in the active centers of the aspartic endopeptidases. Metalloendopeptidases use a metal ion in the catalytic mechanism, and this metal ion is usually, but not always, Zn2 + ion [7].

Table 2.4 The EC system of classification of peptidases [7]

Sub-subclass	Type of peptidase
3.4.11	Aminopeptidases
3.4.13	Dipeptidases
3.4.14	Dipeptidyl-peptidases
3.4.15	Peptidyl-dipeptidases
3.4.16	Serine-type carboxypeptidases
3.4.17	Metallocarboxypeptidases
3.4.18	Cysteine-type carboxypeptidases
3.4.19	Omega peptidases
3.4.21	Serine endopeptidases
3.4.22	Cysteine endopeptidases
3.4.23	Aspartic endopeptidases
3.4.24	Metalloendopeptidases
3.4.99	Endopeptidases of unknown type

Proteolytic enzymes and inhibitors of these enzymes; Control of cell cycle, cell growth, differentiation, and critical metabolic activities that maintain the continuity of the life of the organism such as apoptosis, gene expression, enzyme modification, immune reactions, tissue shaping. The inhibition of proteases by specific proteins synthesized in the cell is one of the most important control mechanisms regulating protease activity in living organisms. Inhibition of proteolytic enzymes by peptides or organic structured inhibitors obtained from natural sources or by synthetic means can result in the death of invasive pathogens. This information has contributed to the development of new types

of antibiotics. The formation of enzyme-inhibitor complexes can be sensitively monitored by conformational changes and by changes in fluorometric data obtained from fluorescently-encoded amino acids or by fluorescently-labeled inhibitors, including the reaction kinetics protein. Adaptation of recently synthesized inhibitors to fluorescence technique makes it possible to monitor enzyme activity using more sensitive methods [8,9].

2.5.1 Chymotrypsin(E.C.3.4.21.1)

It is a digestive enzyme and one of the serine proteases . All serine proteases have three residues : histidine , serine, and aspartate in ther active site , in chymotrypsin the residues are (His^{57} ,Ser^{195}, and Asp^{102}) according to the numbering system. Chymotrypsin synthesized from the acinar cells of the pancreas as an inactive precursor structure called chymotrypsinogen (Figure 2.11). This precursor structure is proteolysis by trypsin to separate into two pieces include deletation of residues 12-15 and 147-148 , these two pieces are not fully separated as they are still linked to each other by a disulfide (-S-S-) bond. These two pieces , activate each other by separating small peptide fragments from each other by a mutual hydrolysis mechanism called trans-proteolysis. Ultimately produces an effective chymotrypsin enzyme. This enzyme hydrolytically cleaves peptides by the carboxyl of the amino acids tryptophan, tyrosine, phenylalanine, leucine and methionine [8, 9 ,28].

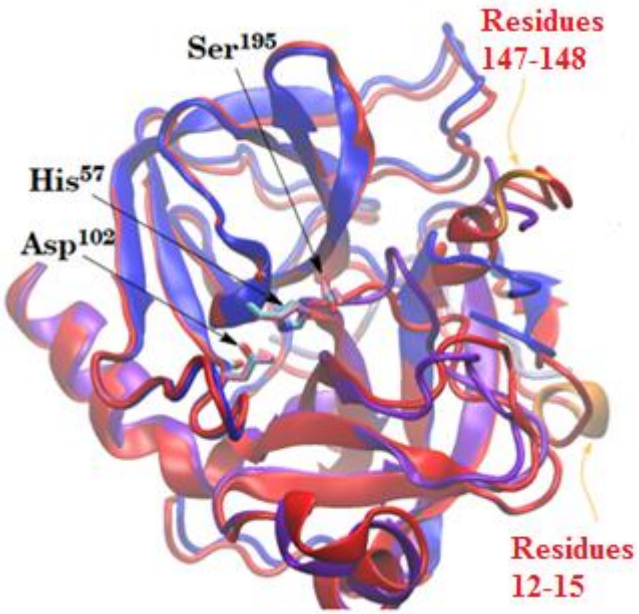

Figure 2.11 Structures of chymotrypsin and chymotrypsinogen [28]

2.6 Catalytic Mechanism of Serine Proteases

Based on their structural properties, serine proteases are classified in three classes; Chymotrypsin-like, Subtilisin-like and Carboxypeptidase II-like. These three classes are quite different from each other in terms of secondary and tertiary protein structures. The main factor of the catalytic mechanism is the **catalytic triad** which consists of three amino acids (a histidine ,a serine and an aspartate), those located in the active site of serine protease. All Serine Proteases perform peptide and ester bond hydrolysis by applying the same acyl transfer mechanism [19 , 28].

The steps of catalytic mechanism:

1) Substrate binding: The side-chain of the amino acid residue immediately before the scissile peptide bond can bind to the recognition site on the enzyme.

2) Nucleophilic attack: Ser^{195} acts as a nucleophile,this nucleophilic attacks the peptide substrate specifically the carbonyl group of this peptide, Produces a covalent bond between oxygen in the side chain of Ser^{195} and carbon in the peptide substrate . This reaction is facilitated by His^{57}. The resulting negative charge on the oxygen is stabilized by the hydrogen bonds formed between hydrogen and nitrogen in the region called "oxyanion hole" because it give stability to the negative charge on the oxygen; the oxyanion hole is very important for catalysis

3) Protonation: His57 give a proton to the substrate amide nitrogen, Making the C-terminal fragment of the substrate release as a free peptide.

4) Ester hydrolysis: In the last step, the water attacked on the ester bond between oxygen in the side chain of Ser195 and the peptide. This generates another Peptide with a normal carboxyl group, and renew the serine hydroxyl. The second peptide is then separated from the enzyme to allow initiation of another catalytic role.

The four steps of catalytic mechanism are in the figure below:

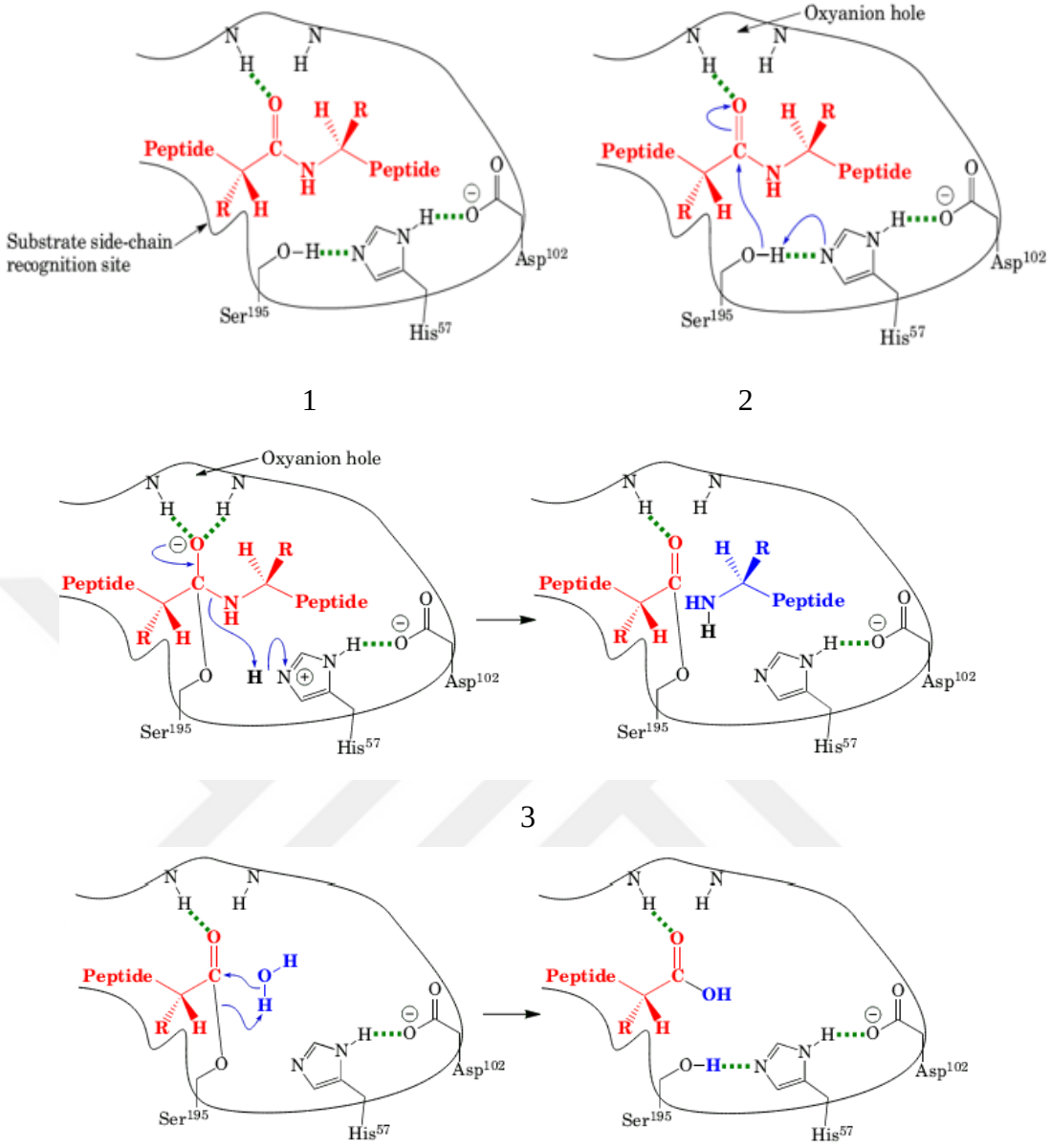

Figure 2.12 Steps of catalytic mechanism of serine protease: **1**) Substrate binding, **2**) Nucleophilic attack, **3**) Protonation, **4**) Ester hydrolysis [28]

The substrate-active site reaction in serine proteases chymotrypsin is seen in (Figure 2.13) [20].

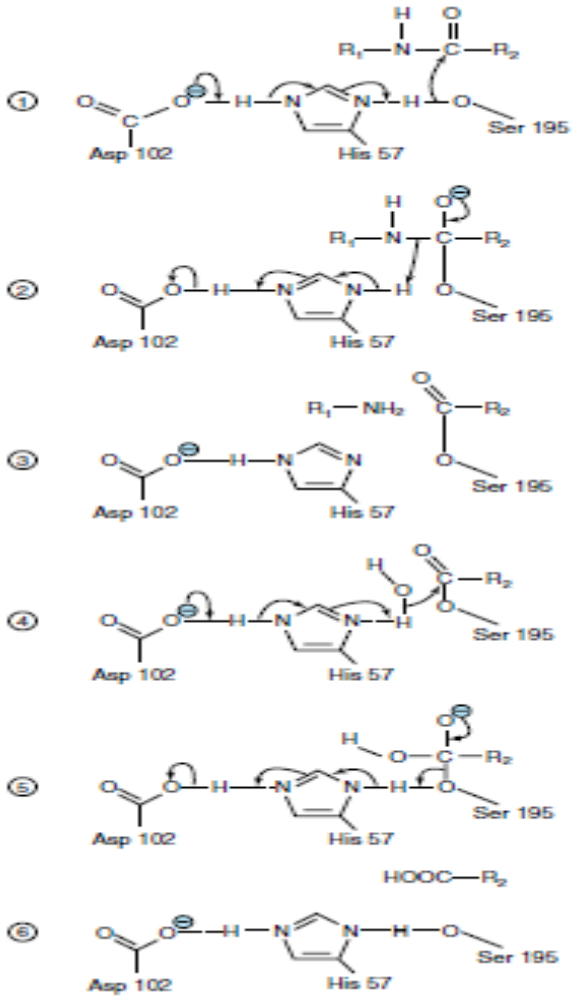

Figure 2.13 Catalyticc mechanism of chymotrypsin [20]

2.7 Enzyme Kinetics

Almost any kind of chemical reaction has an energy barrier called free energy of activation or Gibbs free energy (G)is the energy difference between the free energy of reactants and transition state (T*), where the high-energy intermediate is occur during the conversion of the substrates (A) into the products (B). In order for reaction to occur, molecules must have double energy to pass the energy barrier of the transition state.

$$A \rightleftarrows T^* \rightleftarrows B$$

During the enzymatic reactions, the enzyme allows a reaction to move quickly by providing an alternative reaction pathway with a lower free energy to reach the final state (products) (Figure 2.14) [29].

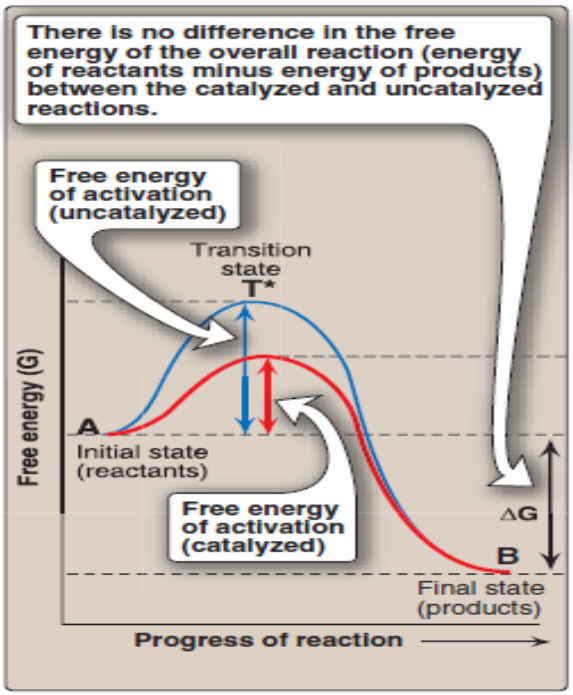

Figure 2.14 Effect of an enzyme on the activation free energy [29]

In 1902, Brown proposed the following reaction mechanism for enzyme catalyzed reactions:

$$E + S \underset{k_{-1}}{\overset{k_1}{\rightleftharpoons}} ES \underset{k_{-2}}{\overset{k_2}{\rightleftharpoons}} E + P \tag{2.1}$$

Assuming that the enzyme is not as specific as the affinity of the product (P) to the substrate (S), it can be assumed that the product formation rate constant k_{-2} from the products is small enough to be neglected ($k_{-2} << k_2$) and the reaction equation can be simplified as follows:

$$E + S \underset{k_{-1}}{\overset{k_1}{\rightleftharpoons}} ES \xrightarrow{k_2} E + P \tag{2.2}$$

There are two important kinetic models developed in order to explain the enzyme kinetics by considering the reaction (Equation 2.2) .

2.7.1 Fast Equilibrium Model

The rate of a reaction, except zero-degree reactions, is proportional to the concentrations of the materials entering the reaction. The fast equilibrium model was first proposed by Henri in 1903 and then developed in 1913 by Michaelis and Menten to give the final

shape. According to this model, a fast equilibrium is established between the reactive substances (E + S) and the ES complex they form and the reaction becomes stable In a short time. If the two-way reaction rates are equal to each other in this fast-established balance :

$$K_1[E][S] = K_{-1}[ES] \tag{2.3}$$

The conversion of the ES complex to the products in the front direction is slower than the free enzyme and substrate conversion In the rear direction ($k_2 << k_1$ and k_{-1}). The dissociation constant k_s of the ES complex to the reaction products (E and S reagents) is written as follows :

$$K_s = \frac{[E\ ][S]}{[ES]} = \frac{k_{-1}}{k_1} \tag{2.4}$$

E: consntrtion of Free enzyme, S: consntration of substrate, ES: Enzyme-substrate complex , K_S: dissociation constant of the ES.

The total concentration of enzyme [E_0] must be the sum of the concentration of free enzyme [E] and the concentration of bound enzyme [ES] .

$$[E] = [E_0] - [ES] \tag{2.5}$$

If we replace the term [E] in equation 2.4 with the term[E] in equation 2.5

$$K_s = \frac{([E_0] - [ES])[S]}{[ES]} \tag{2.6}$$

And if we leave the term [ES] alone on the left side in equation 2.6,

$$[ES] = \frac{[E_0][S]}{K_s + [S]} \tag{2.7}$$

In the reaction equation 2.2, the speed of the entire reaction relative to the rate determining step at which the ES complex is turned into products according to this relationship:

$$V_0 = K_2[ES] \tag{2.8}$$

If we replace the exponent of the term [ES] in 2.7 with the equivalent in 2.8, we obtain:

$$V_0 = K_2 \frac{[E_0][S]}{K_s + [S]} \tag{2.9}$$

When the substrate is saturated with the enzyme in the reaction medium, the total enzyme concentration is equal to the Enzyme-Substrate complex concentration ($[E_0] = [ES]$) and the reaction rate reaches its maximum when no free enzyme is expected to be present and the substrate concentration is very high so all the Enzyme is present as the Enzyme-Substrate complex and the limiting initial velocity (V_{max}) is reached as :

$$V_{max} = K_2[E_0] \tag{2.10}$$

And this equation is replaced by the equation 2.9

$$V_0 = \frac{V_{max}[S]}{K_s + [S]} = \frac{V_{max}}{1 + \frac{K_s}{[S]}} \tag{2.11}$$

Equation 2.11 is the final kinetic expression of Henri, Michaelis and Menten independently .

2.7.2 Steady State Model

The British biologists George Briggs and John Haldane in 1925 explained that the balanced bonding of the enzyme and substrate could be done by a steady state model, that during enzymatic reaction, the rate of [ES] complex formation is stabilized by its rate of decomposition to free enzyme and product; [(d [ES] / dt) = 0]. After mixed the substrate and the enzyme, a rapid accumulation of the [ES] complex in a pre-steady state, followed by a long period of time at which the concentration of [ES] complex does not change, and lastly a post—steady state step i where a large amount of substrate is exhausted.

For this reason, the proposed model does not require $k_2 << k_{-1}$ accepted in the Henri-Michaelis-Menten model.

Considering the reaction equation 2.2, the rate of ES complex formation according to the steady state model,

$$\frac{d[ES]}{dt} = K_1[E][S] \tag{2.12}$$

And the rate of destruction of the ES complex

$$\frac{-d[ES]}{dt} = (K_{-1} + K_2)[ES] \tag{2.13}$$

Since the formation and demolition rates in equilibrium will be equalized

$$K_1[E][S] = (K_{-1} + K_2)[ES] \tag{2.14}$$

For this equation [ES]:

$$[ES] = \frac{[E][S]}{\frac{K_{-1} + K_2}{K_1}} \tag{2.15}$$

It can be rearranged in the form of The fractional expression

$$K_m = \frac{K_{-1} + K_2}{K_1} \tag{2.16}$$

Where (K_m) is Michaelis constant

We can simplify equation 2.15 as follows

$$[ES] = \frac{[E\ ][S\ ]}{K_m} \tag{2.17}$$

If the term ES is substituting in equation 2.5

$$[ES] = E_0 \frac{[S]}{[S] + K_m} \tag{2.18}$$

If the expression 2.18 is written in place of the speed Equation 2.8, which is based on the determining step,

$$V_0 = k_2[E_0]\frac{[S]}{[S] + K_m} \tag{2.19}$$

We get equal. equation 2.19; Instead of K_2, we can generalize as follows by expressing K_{cat} that is the catalytic step velocity constant :

$$V_0 = K_{cat}[E_0]\frac{[S]}{[S] + K_m} \tag{2.20}$$

The fractional term of this expression is equal to the limit of 1 according to L'Hospital's Rule when the substrate concentration goes to infinity.

$$\lim_{[S]\to\infty} \frac{[S]}{[S] + K_m} = \frac{\infty}{\infty} \Rightarrow \lim_{[S]\to\infty} \frac{([S])'}{([S] + K_m)'} = \lim_{[S]\to\infty} \frac{1}{1} = 1 \tag{2.21}$$

When this result is written in place of Equation 2.20, we get the maximum speed expression given in Equation 2.10.

$$V_{\max} = k_{cat}[E_0] \tag{2.22}$$

By combining Equation 2.22 with Equation 2.20 we arrive at Equation 2.23, very similar to the Henri-Michaelis-Menten model

$$V_0 = \frac{V_{\max}[S]}{K_m + [S]} = \frac{V_{\max}}{1 + \frac{K_m}{[S]}} \tag{2.23}$$

Equation 2.23 is the fundamental equation of the steady-state enzyme kinetic model.

Equation to the left of equation 2.24, which indicates that V_0 velocity reaches half of maximum velocity

$$V_0 = \frac{V_{max}}{2} \tag{2.24}$$

When the counterpart of 2.23 is written, the equation 2.25 is obtained

$$\frac{V_{max}[S]}{K_m + [S]} = \frac{V_{max}}{2} \tag{2.25}$$

If this equation is refined by simplification

$$K_m = [S] \tag{2.26}$$

This result; Which is equal to the K_m value of the substrate concentration corresponding to half of the maximum velocity [19,20,26, 30,31].

2.8 Covalent Bioconjugation

In biconjugation chemistry, covalent reaction is used to bind two biomolecules with each other or biomolecules with small molecules by covalent bond to form new significant molecules (Figure 2.15). The reactive molecules (proteins, peptides, carbohydrates, nucleic acids, etc.) have specific reactive functional groups include (carboxylic acids, aldehydes, ketones, amines, thiols, and alcohols), which are generally present or can be instituted into molecule.

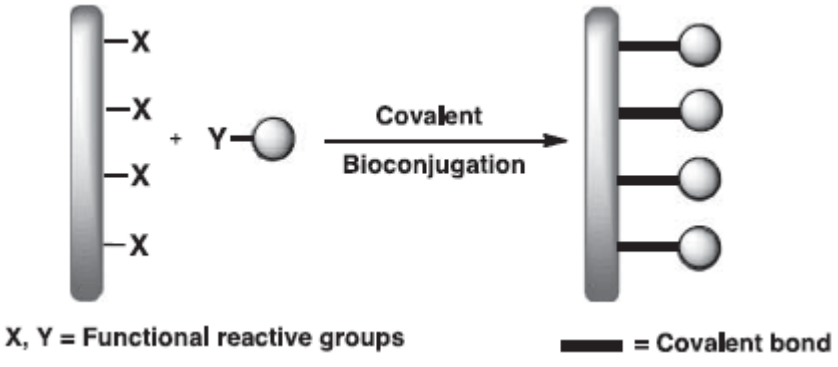

Figure 2.15 Schematic representation of covalent bioconjugation strategy [16]

Bioconjugation is a burgeoning field of research that encompasses a wide range of science between chemistry and biology [16]. It has made Possible to find new biomolecules, Clarification of complex biological processes and also used in the medical, diagnostics life sciences, microelectronics, and material sciences fields. In a medical point, often development of drugs depends on the Highly specific bioconjugates with therapeutic efficacy toward certain cells, tissues or disease states. Many of the largest pharmaceutical companies have started to rely on bioconjugation to design their future products and maintain vital competition [17].
Ther are many types of bioconjugates, such as (protein–protein, polymer– Protein and carbohydrate–protein).

In this study we used polymer-protein Bioconjugation

2.8.1 Bioconjugation of Polymers with Proteins by Using EDC

Protein–polymer conjugates are biohybrid materials and can combine the advantages of both components and avoid the disadvantages of each separate component. For example, proteins may acquire a higher chemical and thermal stability in their conjugated forms with polymers. In the process of protein conjugation with the polymer, an immobilized reagent 1-Ethyl-3-(3-dimethylaminopropyl) carbodiimide (EDC) derivative of Carbodiimides (CDI), it is commonly known as a zero-length cross-linking agent used to conjugate a carboxylate in one molecule to an amine in another molecule by covalent amide bond. EDC reacts with carboxylic acid first and activates the carboxylate group to form an active intermediate ester (O-acylisourea) soluble in water, the carbonyl group of this ester attacked by the amine compound to results an amide bond and release of an isourea (Figure 2.16) [17,18].

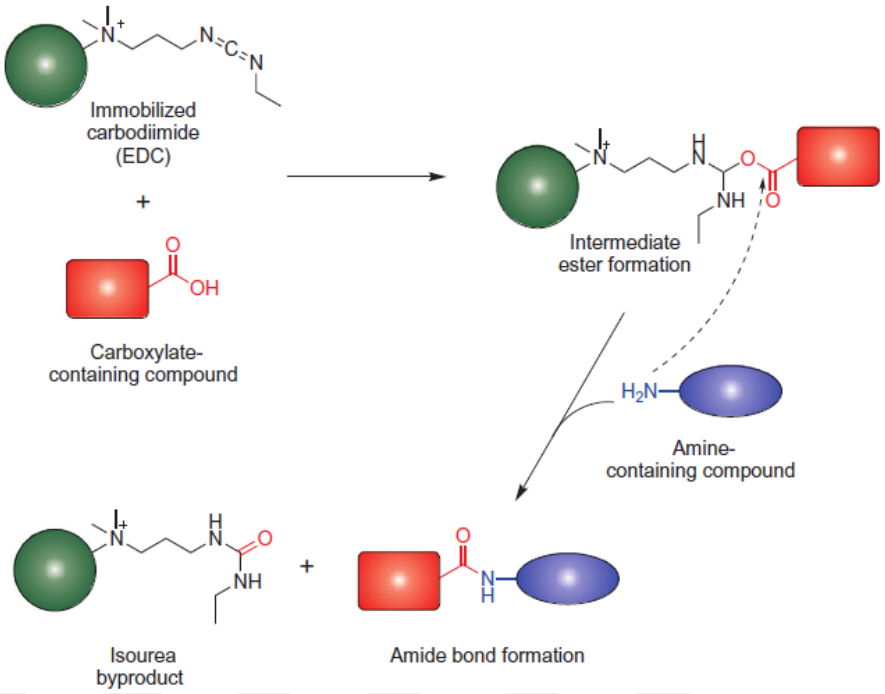

Figure 2.16 Conjugation of two molecules containing a carboxylate and an amine groups by using EDC to form an amide bond [18]

2.9 Spectrophotometric Methods Used to Determine Enzyme Activity

Determination of K_m and K_{cat} kinetic constants of an enzymatic reaction; Based on the ability to accurately measure the initial rate of reaction under well-controlled conditions. The velocity of enzymatic reaction is highly sensitive to such factors such as pH, temperature and solvent components, and this requires full control of the agents in order to obtain meaningful data from the activity assay method used.

In order to measure the reaction velocity; it is needed to follow the signal corresponding to the amount of product formed with time or the amount of substrate decreasing with time. In general, progress of the reaction is monitored in most enzyme assays by using many identification and separation methods: (**Spectroscopy, Polarography, Radioactive decay, Electrophoretic separation, Chromatographic separation, Immunological reactivity**) [19].

In this chapter, "Ultraviolet-Visible Absorption Spectroscopy" and "Fluorescence Spectroscopy" and "Gel Filtration Chromatography" will be considered as the methods of activity determination which are important for our study

2.9.1 Ultraviolet-visible Spectroscopy

Photons with certain energy, they are absorbed by the atoms or electrons of the molecules that collide with them, and at this time the electrons are emitted to the upper energy levels. Absorption spectroscopy is performed with devices designed to determine the wavelengths and absorbance of this absorption. Ultraviolet-visible region Absorption spectroscopy, it examines the absorption properties of substances corresponding to wavelengths in the ultraviolet and visible regions of the electromagnetic spectrum. Absorption spectroscopy is important as an analytical tool to determine the presence of a specific substance in a sample, and in many conditions, to quantify the concentration of the substance into the medium.

the sample is put in a cuvette, the light beam enter to the monochromator and exit with single wavelength and passes through the cuvette, some light is absorbed by the sample, and unabsorbed or transmitted light is recorded by the spectrophotometer (Figure 2.17).

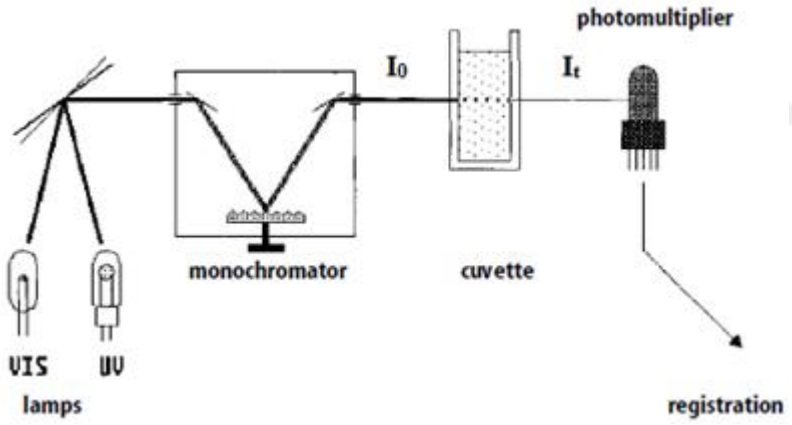

Figure 2.17 General schematic of a spectrophotometer [30]

To remove reflections and distractions, glass rectangular cuvettes with ground surfaces are used. Its thickness about 1cm, in the range of a visible spectrum (340–800 nm).

The ratio of the intensity of the beam of light after passing through the sample (transmitted light) to the intensity of the beam of light before encountering the sample (incident light) called as Transmittance and determined by the equation:

Transmittance: $T = \frac{I_t}{I_0}$ (2.27)

I_t : transmitted light , I_0 : incident light

We can convert this ratio into a percentage by multiplying by 100 to get Percent Transmittance ($\%T$):

% Transmittance: $\%T = \frac{I_t}{I_0}.100$

(2.28)

The Absorbance to measure how much light is absorbed by sample it is given by the following equation:

$$A = -\log T = -\log \frac{I_t}{I_0} \quad (2.29)$$

The relationship between the absorption of the sample through which light passes and the concentration of the substance in a sample is explained by the Lambert-Beer law:

$$A = \varepsilon cl \quad (2.30)$$

A: Sample absorbance at a given wavelength (no unit)

ε: Molar absorptivity $M^{-1} \cdot cm^{-1}$

c: Sample molar concentration (M)

l: the path length of sample the light traverses (cm) [3,19,30].

According to the Lambert-Beer law, the absorption of the sample increases linearly with the analyte concentration. In general, when the concentration increases to the reading at which A=1.0, the large deviations will appear in the straight line. Therefore, the concentration of a substance to be subjected to kinetic analysis in the solution is generally adjusted to give an absorbance of (0.05-1.0) (Figure 2.18).

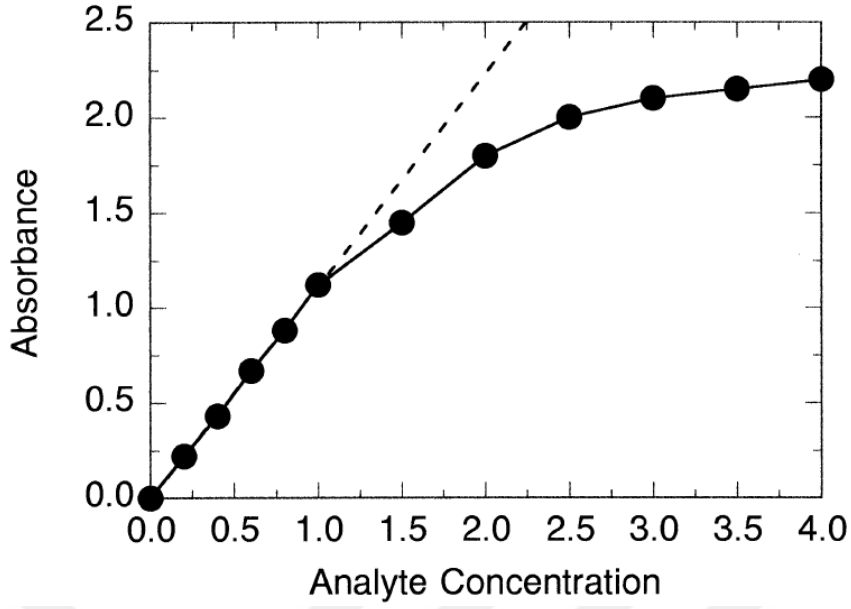

Figure 2.18 Deviation from the Lambert-Beer law [19]

Selection of analytical wavelength to be used to determine enzyme kinetics; should be in a wavelength provide the greatest difference in absorption between both of substrate and product molecules, that to avoid spectral overlap. The wavelength chosen for the substrate and product is typically the wavelength maximum for each molecule [19].

2.9.2 Fluorescence Spectroscopy

Fluorescence is an emission phenomenon where an energy transition from a higher to a lower state is accompanied by radiation. Only molecules in their excited forms are able to emit fluorescence; thus, they have to be brought into a state of higher energy Prior to the emission phenomenon. The processes that occur between the absorption and emission of light are usually illustrated by the Jablonski diagram (Figure 2.19), a molecule in its electronic and vibrational ground state (S_0V_0) can absorb photons matching the energy difference of its various discrete states. The required photon energy has to be higher than that required to reach the vibrational ground state of the first electronic excited state (S_1V_0). The excess energy is absorbed as vibrational energy ($V>0$), and quickly dissipated as heat by collision with solvent molecules, molecule thus returns to the vibrational ground state(S_1V_0). These relaxation processes are non-radiating transitions from one energetic state to another with lower energy, and are called internal conversion (IC). From the lowest level of the first electronic excited state, the molecule returns to the ground state (S_0) either by emitting light (fluorescence)

or by a non-radiative transition. Upon radiative transition, the molecule can end up in any of the vibrational states of the electronic Ground state, most molecules are flexible and thus have very high vibrational levels in the ground state. Since radiative energy is lost in fluorescence as compared to the absorption, the fluorescent light is always at a longer wavelength than the exciting light. The emitted radiation appears as band spectrum, because there are many closely related wavelength values dependent on the vibrational and rotational energy levels attained. The probability of the transition from the electronic excited to the ground state is proportional to the intensity of the emitted light, an associated phenomenon in this context is phosphorescence which arises from a transition froma triplet state (T_1) to the electronic (singlet) ground state (S_0).

The molecule gets into the triplet state from an electronic excited singlet state by intersystem crossing (ISC). The transition from singlet to triplet is quantum-mechanically not allowed and thus only happens with low probability in certain molecules where the electronic structure is favorable, such molecules usually contain heavy atoms. The rate constants for phosphorescence are much longer and phosphorescence thus happens with a long delay and persists even when the exciting energy is no longer applied [32].

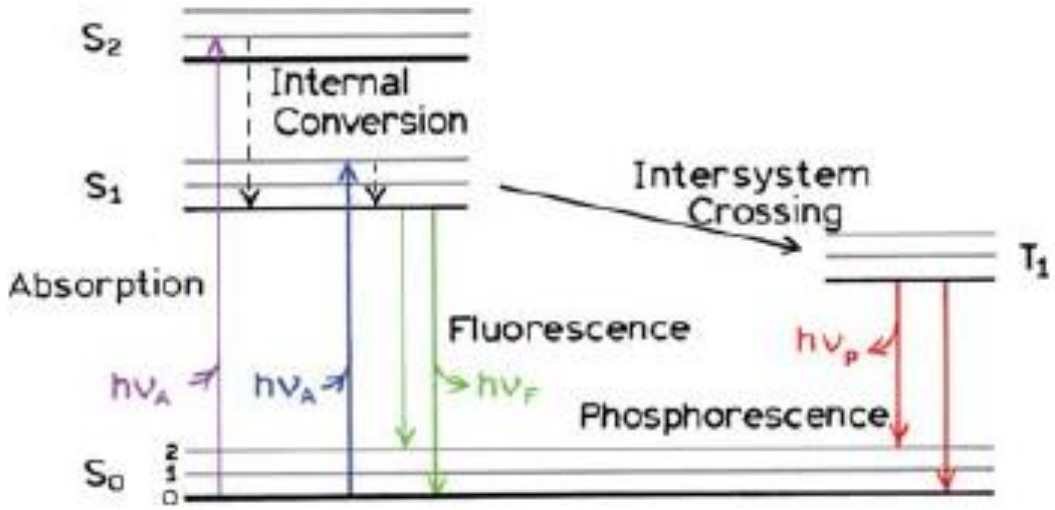

Figure 2.19 Jablonski diagram. (S_0) : the electronic ground state , (S_1, S_2) : two excited singlet states , (T_1) : triplet state , (v) : Vibrational levels , (ISC) : intersystem crossing , (IC) : internal conversion [2]

In the figure up; Solid vertical lines indicate radiative transitions, dotted lines show non-radiative transitions. The Absorption occur is about 10^{-15} s, a time too short for significant displacement of nuclei. Vibrational relaxation occurs between 10^{-12}-10^{-10} s .Since fluorescence lifetimes are typically near 10^{-8}s. The intersystem crossing and phosphorescence require a spin reorientation. Therefore, absorption and fluorescence are much faster than phosphorescence .Phosphorescence is a long transition that can last from milliseconds to seconds, it occur abut 10^{-6} s^{-1}. Internal conversion occur between 10^{-11}-10^{-9} s [2-4].

The fluorescence properties of a molecule are determined by properties of the molecule itself (internal factors), as well as the environment of the protein (external factors). The fluorescence intensity emitted by a molecule is dependent on the lifetime of the excited state. The number of molecules in the excited state decreases exponentially with time [32].

Due to the different core spacings of the in-atom base and excited states and due to energetic losses as they pass through the higher energetic vibrational subdivisions during the fundamental transformation phase, $E = hc / \lambda$ [E: energy, h: Planck constant (6, 62x10-34 js-1), c: speed of light, λ: wavelength of the photon emitted by the electron as it turns to the ground state is lower than that of the exciting photon]. The wavelength of emissivity was first named "Stokes shift" in 1852 because it was watched by George G. Stokes. Due to solvent effect and excited reactions, stokes shift can be observed at relatively longer wavelengths (Figure 2.20) [2-4,33] .

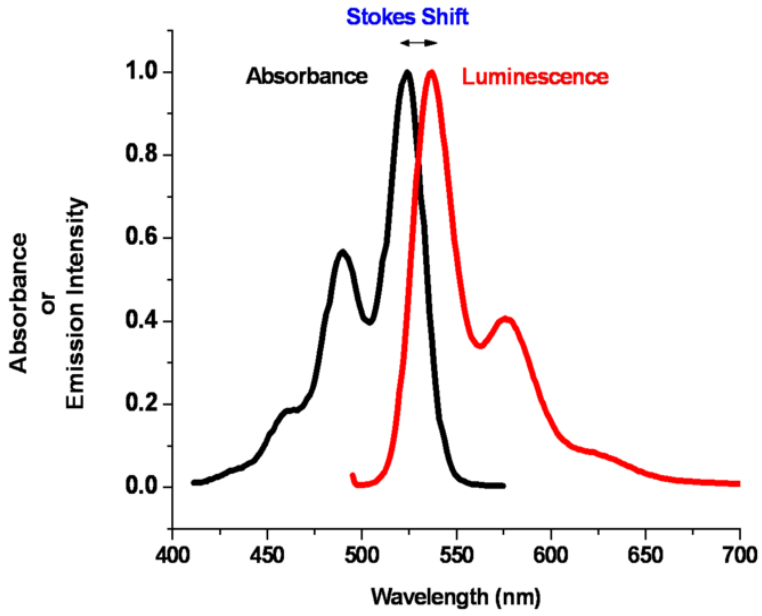

Figure 2.20 Stokes shift. Luminescence occurs at longer wavelengths than Absorbance [33]

A large number of enzyme substrates or enzymatic reaction products exhibit natural fluorescent character and produce suitable fluorescence signals in the reaction process to ensure that they do not run out or form in solution. If these molecules do not exhibit fluorescence properties, fluorescence derivatives can be formed by attaching fluorescent groups to structures under covalent bonds, without significantly disturbing their interaction with the enzyme under operating conditions. Fluorescence signals show a linear quantitative relationship with the concentration of fluorescent substance at a limited concentration. Fluorescence signals vary in intensity with the concentration of the fluorescent substance in a similar relation to the Lambert-Beer law, where the Absorption (A) is replaced by Quantum yield (Q_f). Quantum yield is the ratio of the amount of emitted photons to the amount of absorbed photons.

$$Q_{f=}\frac{\text{fluorescence intensity of emitted photon flux } (I_f)}{\text{absorptive photon}(I_a)} \tag{2.31}$$

Here, $I_a = I_0 - I_t$ (2.32)

I_0: the sample enviromen

I_t: Light intensity at the sample environment

Since the $I_t = I_0 \times 10^{-\varepsilon bc}$ (2.33)

And write this expression in place of the expression 2.32

$$I_a = I_0 \times (1 - 10^{-\varepsilon bc}) \quad (2.34)$$

We get equal. Using the equations 2.31 and 2.33

$$I_f = Q_f \times I_a = Q_f \times I_0 (1 - 10^{-\varepsilon bc}) \quad (2.35)$$

We obtain the equation giving the relation between fluorescence intensity and fluorescence substance concentration [5].

In equation 2.35 . The terms(I_0,ε and b) are usually the same for both unknown and standard samples under certain conditions. the expression can be expanded (Taylor series) as follows.

$$I_f = Q_f \times I_0 [2.3\varepsilon bc - \frac{(2.3\varepsilon bc)^2}{2!} + \frac{(2.3\varepsilon bc)^3}{3!} - \cdots] \quad (2.36)$$

If εbc is small (≤0.05) we obtain :

$$I_f = 2.3 \times Q_f \times I_0 \varepsilon bc \quad (2.37)$$

The equation 2.37 gives the intensity of fluorescence.

Here is the value of (I_f) ; It is understood that absorptive species (basal species) are related to fluorescence quantum yield (Q_f) by molar absorptivity (ε) and fluorescence emitting species (induced species). Under certain excitation conditions, (I_f) , (Q_f) , (ε) and (b) are usually the same for unknown and standard samples. Utilizing this, the following proportional relationship between the concentrations of unknown and standard specimens and fluorescence intensities can be established.

$$\frac{I_{f_b}}{I_{f_s}} = \frac{C_b}{C_s} \quad (2.38)$$

Where (I_{f_b}) and (I_{f_s}) are the experimentally determined fluorescence intensities of unknown and standard samples; (C_b) and (C_s) are concentrations [5, 34].

Fluorescence spectroscopy is generally classified in two methods:

(1) Steady state fluorescence spectroscopy

(2) Time Resolved Fluorescence Spectroscopy

In this study we used Time Resolved Fluorescence method

2.9.2.1 Steady -State Fluorescence Spectroscopy

Steady-state measurements are those performed with constant illumination and observation. The sample is illuminated with a continuous beam of light, and the intensity or emission spectrum is recorded. The general optical scheme for steady-state fluorometers is shown in (Figure 2.21) [2, 35].

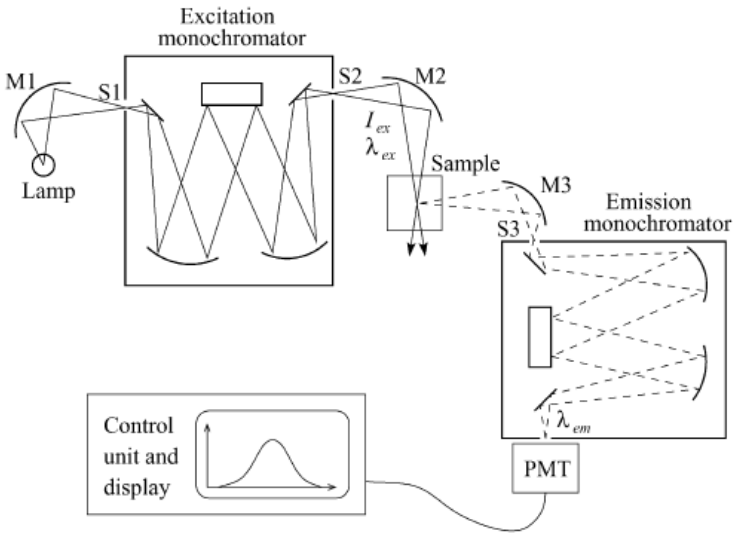

Figure 2.21 An optical scheme of a steady state fluorimeter [35]

The emission of the lamp is collected by mirror Ml and focused into the input slit S1 of the excitation channel monochromator. Mirror M2 collects the light from the monochromator output (slit S2) and focuses it into the sample. Emission of the sample is collected by mirror M3 and directed to the input slit S3 of the detection monochromator. The light intensity is measured by a photomultiplier tube (PMT).

Naturally, for the emission spectrum measurements, λ_{em} is kept constant. The sample concentration is fixed, does not change with time, and therefore the method referred to as the steady state means that the molecules in the excited state undergo nanosecondary or shorter time scales [2, 35].

2.9.2.2 Time Resolved Fluorescence spectroscopy

Time-resolved measurements can be performed at nanoscale or smaller time scales, so it commonly used in fluorescence spectroscopy. To measuring time-resolved fluorescence use stroboscopic pulse sampling technique, in this technique the sample is excited with a pulse light source. The intensity of the fluorescence emission is measure in a very narrow time Window on each pulse and save in the computer. The time window is move after each Pulse. When samples are taken from the data over the appropriate range of time, decay Curve of emission intensity versus time can be constructed. The name "strobe technique" comes about because the photomultiplier PMT is gate or strobe by a voltage pulse that is synchronize with the pulse light source. The strobe has the effect of "turning on" the PMT and measuring the emission intensity over a very short time window (Figure 2.22) [2, 36].

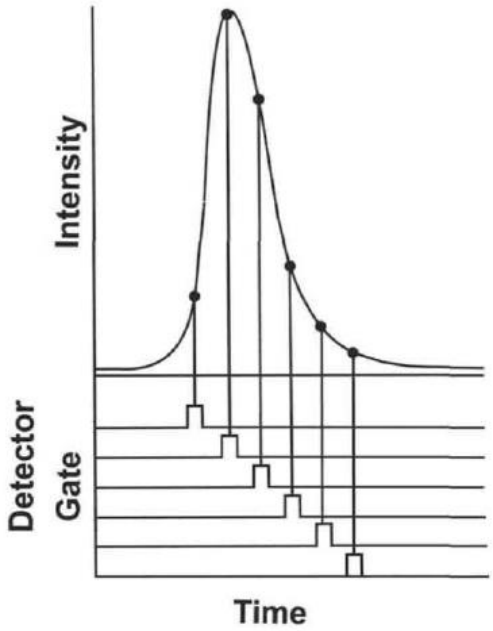

Figure 2.22 Schematic profile of the fluorescence lifetime measured with the Strobe method [36]

The fluorescence decay data analysis by using the exponential series method (ESM) to obtain the changes of lifetime distributions [4].

2.9.2.3 Exponential series method (ESM)

Fluorescence decay can be described as a sum of multi-exponential decays (Equation 2.39) which is consisting of exponential terms with a limited number, discrete and each with a unique fluorescence lifetime (τ). Each term may refer to the decays of local emissions due to discrete environments in the molecule, which have different polarities and are interacting with solvent molecules at different degrees of freedom.

$$F(t) = \sum_{i=1}^{N} a_i \exp(-t/\tau_i) \tag{2.39}$$

F(t): fluorescence decay intensity

τ_i: fluorescence lifetime

α_i: "pre-exponential factor" and $\sum_i a_i = 1{,}0$.

Because of the high number of regions exhibiting polarity diversity in different parts of large and complex molecules such as proteins, the discrete multiple exponential decay analysis does not provide insight into the fluorescence lifetime diversity of proteins by using distributional approach model which describes the fluorescence decay as continuous distributions of fluorophore states [2,3,10,35,37].

In the distributional approach model, integrals replace the exponential sums of exponential terms as seen in (Equation 2.40) , and the forward exponential factors that denote the partial contributions of terms to the total decomposition are transformed into the distributional functions of continuous lifetime variants [a(τ)], that's the reason of its calling as "fluorescence lifetime distributions ,distributed approach model" a specific fluorescence lifetime serves as a partial contribution to total decay [2, 37, 38].

The componet with each indivdual τ value of total decay

$$F(\tau, t) = \alpha(\tau) e^{-t/\tau} \quad (2.40)$$

The total decay: sum of individual decays

$$F(t) = \int_0^{\infty} a(\tau) \exp(-t/\tau)\, d\tau \quad (2.41)$$

where α(τ): distribution functions of the continuous lifetime variable, satisfies the condition $\int a(\tau) d(\tau) = 1.0$.

The function of the lamp pulse, called "Instrument (or Impulse, Pulse, Lamp) Response Function (IRF), L(t)", actually distorts the experimental fluorescence decay intensity, since it has a finite width. Therefore the observed decay is convoluted and its function is known as convolution integral I(t), given in (Equation 2.42) [2,3,39,40].

$$I(t) = \int_0^t L(t) F(t-s) ds \quad (2.42)$$

I(t): observed decay of fluorescence intensity

L(t): instrument response function

In Exponential series method, a series of exponentials (up to 200) is used as a probe function with fixed, logarithmically spaced lifetimes (τi) and variable pre-exponential factors (α_i) in order to analyze the smooth distributions of α_i and τi . Only the α_i values of the research function are repeated continuously (fitting procedure) by iterative reconvolution until the chi-square function reaches the closest value, almost 1 (Equation 2.43) [15,37, 38, 41].

$$C = \left(\frac{1}{n}\right) \sum_{k=1}^{n} \frac{\left(Y_{k_{\exp}} - Y_{k_{calc}}\right)^2}{\sigma_k^2} = \left(\frac{1}{n}\right) \sum_{k=1}^{N} \frac{\left(Y_{k_{\exp}} - \sum_{i=1}^{N} D_{ki} a_i\right)^2}{\sigma_k^2} \approx 1{,}0 \quad (2.43)$$

where Y_{kexp}: Observed fluorescence intensity in the kth channel, n: The number of channels, σ: The standard deviation in the kth channel, D_{ki}: The convolution matrix (Equation 2.44).

$$D_{ki} = \int_0^{t_k} L(t_k - t) \exp\left(\frac{-t}{\tau_i}\right) dt \quad (2.44)$$

2.10 Excimer Structures

Excimers are excited electronic states dimers that only formed where one molecule exists in an excited state and the other molecule is in a ground state. Excimers are often diatomic and are composed of two atoms or molecules that would not bond if both were in the ground state such as pyrene. Monomer emission of pyrene occurs within the range of 370-390 nm whereas, the excimer emission is obtained within the wavelength limit of 465-500 nm (Figure 2.23) [42,43].

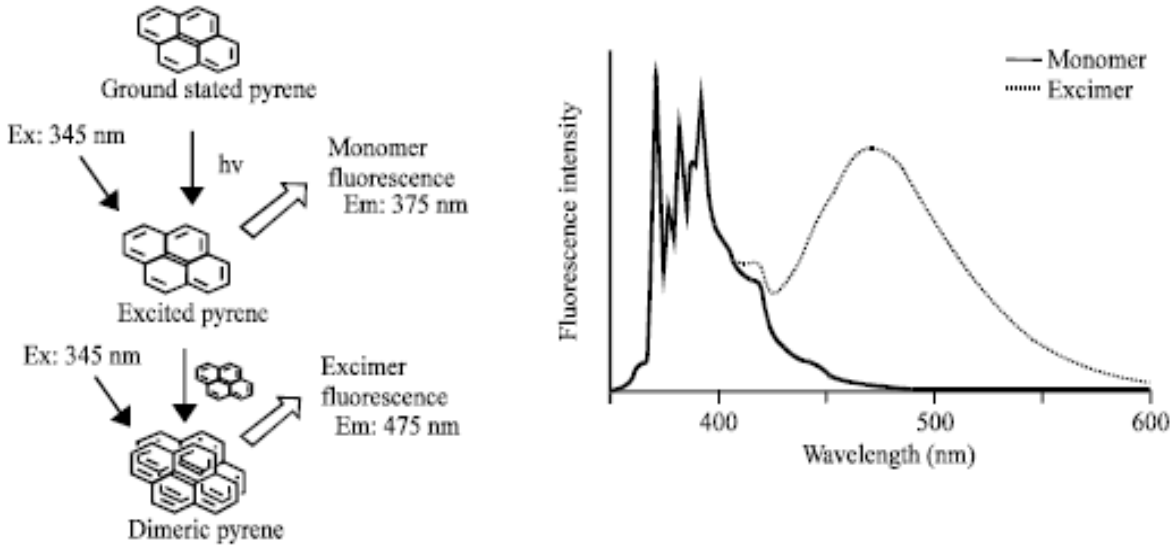

Figure 2.23 Excimer formation by pyrene. Ex: Excitation, Em: Emission [43]

The formation of the eximer takes place in two ways. The first is the encounter with the neutral neutralized partner of a neutral basic monomer. The second is that, in essence, the end result of the radical anion meeting the radical cation at its base. The monomer and excimer fluorescence of a solution depends on the collision rate and the distance between the molecules. The distance between the groups forming the excimer is 0.3 nm or less. Utilizing these properties, it is possible to develop peptide substrates with eximer fluorescent properties for proteolytic enzymes [12 ,42, 44,45].

2.11 Gel Filtration Chromatography (GFC)

The evolution of gel filtration as a method for sizing biopolymers according to their hydrodynamic volume and molecular weight started in 1959, when Porath and Flodin developed cross-linked dextrans as size exclusion chromatography (SEC) packings and advocated the novel technology". This method is used in biochemistry studies for peptides, proteins, DNA fragments, enzymes and so on. Gel filtration is a special type of partition chromatography in which separation is based on their molecular size and shape through a gel filtration medium packed in a column . The separation of the components in the sample mixture, with some exceptions, correlates with their molecular weights. In these cases, gel filtration can be used as an analytical method to determine the molecular weight of an uncharacterized molecule [46].

2.11.1 Protein Purification by Gel Filtration Chromatography

Gel Filtration Chromatography is a non-binding method, (which means that no concentration of the sample components takes place). The basic principle of size exclusion chromatography is quite simple. A column of gel particles or porous matrix is in equilibrium with a suitable mobile phase for the molecules to be separated. Sephadex, Sepharose, and Bio-gel are commonly used commercial preparations of these beads, which are typically 100 mm (0.1 mm) in diameter. Large molecules are completely excluded from the pores and pass through the space in between the gel particles or matrix and come first in the effluent. Smaller molecules get distributed in between the mobile phase of in and outside the molecular sieve and then pass through the column at a slower rate, thus appear later in effluent (Figure 2.24). The loaded sample volume must be kept small. Even larger samples volumes can be suitable if the resolution between target protein and the impurities to be removed is high. Select a buffer that supports protein stability and activity [25] .

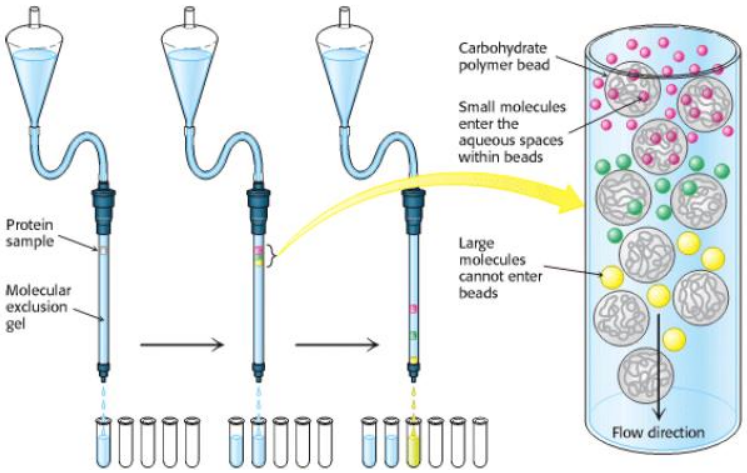

Figure 2.24 Purification of protein by Gel Filtration Chromatography [25]

There are two extremes in the separation profile of a gel filtration column. There is a large mass which will be **completely excluded** from the gel filtration beads. Small mass which will be **completely included** within the pores of the gel filtration beads. The Solutes between these two ranges of molecular mass will elute between the excluded and included volumes (Figure 2.25) [47].

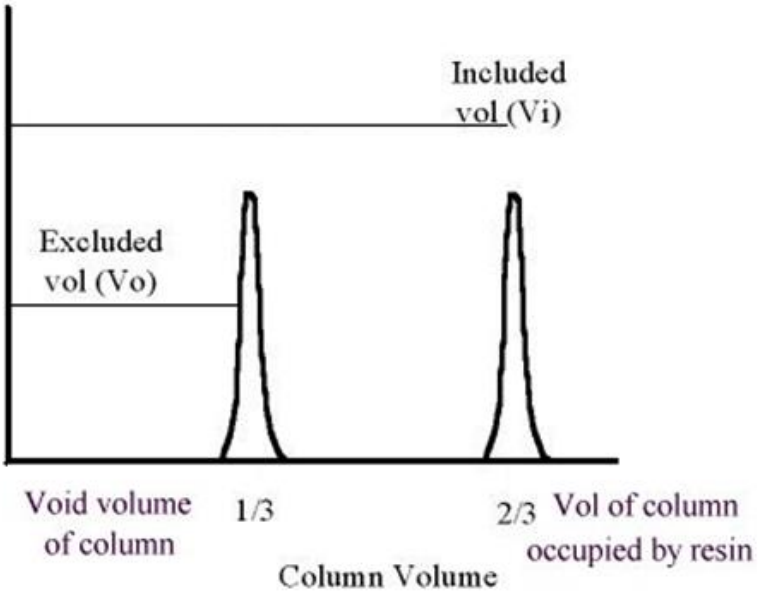

Figure 2.25 The two extremes in the separation profile of a gel filtration column [47]

The excluded volume (V_o) is approximately equal to one third of the column volume, the included volume (V_i) is approximately equal to two thirds of the column volume.

2.11.2 Mechanism of Gel Filtration Chromatography

gel filtration chromatography is a case of liquid-liquid partition chromatography, in which the solute molecules are get distributed in between two liquid phases, (i) liquid in the gel pores and (ii) liquid outside the gel. The gel filtration explained by **Steric Exclusion Mechanism**. As the gel particles contains range of pore sizes, small molecules can enter in large number of pores while the large molecules will get small number of pores into which they can enter. Thus the different fractions of total pore volume are accessible to molecules of different sizes. Thus, molecules with different sizes will differ in distribution coefficient between these two liquid phases [As the small molecules can enter in more pores while larger molecules can enter in pores only larger than the molecular size] [47].

The total volume (V_t) of a column packed with a gel that has been swelled by solvent is given by

$$V_t = V_g + V_i + V_0 \qquad (2.45)$$

V_g : is the volume occupied by the solid matrix of gel

V_i : is the volume of solvent held in the pores or interstices

V_0: is the free volume outside the gel particles

When mixing or diffusion occurs, the diffusion equilibrium and the retention volume (V_R) of the given species is given by

$$V_R = V(_{int.}) + K_d\, V(_{int.}) \qquad (2.46)$$

where distribution coefficient (K_d) is given by

$$K_d = V_i(_{acc}) / V(_{total}) \qquad (2.47)$$

$V_i(_{acc})$: is the accessible pore volume

$V(_{total})$: is the total pore volume

$V(_{int.})$: is the interstitial volume

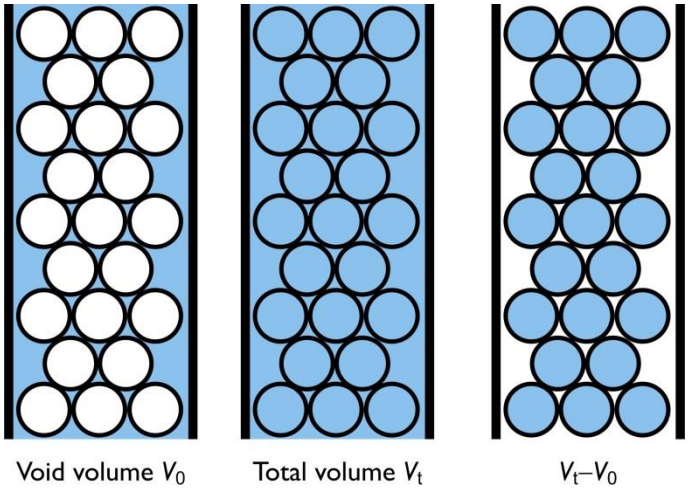

Figure 2.26 Volume definition in gel filtration column. $V_t - V_o$ include the volume of the solid material which forms the matrix [48]

2.12 Reactive Protein Groups and Their Modifying Agents

The chemical reactivity of proteins depend on the side chains of their amino acid compositions as well as the free amino and carboxyl groups of the N- and C-terminal residues, respectively. The terminal residues, however, contribute little of significance to chemical modification since they are of limited number compared to the overall large number of amino acids in the protein [49]. Of the 20 amino acids, the alkyl side chains of the hydrophobic residues are for all intents and purposes chemically inert. Since aliphatic hydroxyl groups of serine and threonine can be considered as water derivatives and therefore have a low reactivity. Only eight of the hydrophilic side chains are chemically active (Table 2.5) [50].

Table 2.5 Chemical reaction of active side chains [50]

Amino Acid	Active Side Chain	Alkylation or Arylation	Acylation	Oxidation	Other Reactions[a]
Cysteine	$-CH_2SH$	+	+	+	a,d,f,h
Lysine	$-NH_2$	+	+	–	c,e,g
Methionine	$-S-CH_3$	+	–	+	i
Histidine	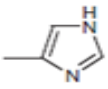	+	+	+	a,c
Tyrosine	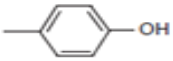	+	+	+	a,b,c,d
Tryptophan	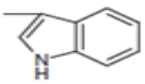	+	–	+	h
Arginine	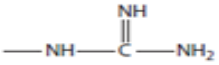	–	–	–	g
Aspartic and glutamic acid	–COOH	–	+	–	d,e

[a] Other reactions include (a) iodination, (b) nitration, (c) diazotization, (d) esterification, (e) amidation, and reaction with (f) mercurials, (g) dicarbonyls, (h) sulfenyl halides, and (i) cyanogen bromide.

The guanidinyl group of arginine, the β- and γ-carboxyl groups of aspartic and glutamic acids, respectively, the sulfhydryl group of cysteine, the imidazolyl group of histidine, the ε-amino group of lysine, the thioether moiety of methionine, the indolyl group of tryptophan, and the phenolic hydroxyl group of tyrosine. The most important reactions are alkylation and acylation. In alkylation, an alkyl group is transferred to the nucleophilic atom, whereas in acylation, an acyl group is bonded. Most protein modifications; Nucleophilic attack reactions involving the removal of an easily cleavable group by nucleophilic reactive groups in the side chains of amino acids (Figure 2.27). The rate of such a bimolecular nucleophilic substitution reaction, the S_N2 mechanism, depends on at least two factors: the ability of the leaving group to leave and the nucleophilicity of the attacking group. The more facilely the leaving group comes off, the faster will be the reaction [51,52].

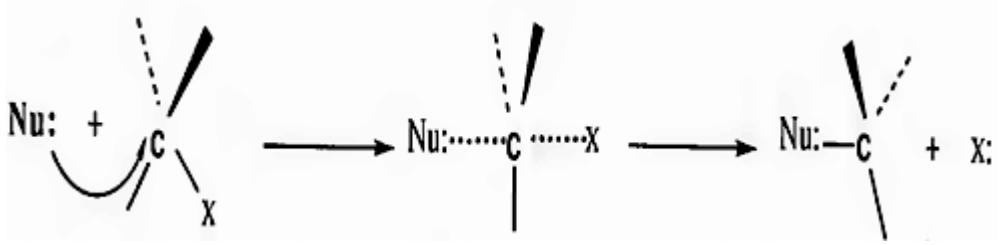

Figure 2.27 The nucleophilic substitution reaction, the SN2 reaction mechanism. The nucleophile (Nu:) attacks an electron-deficient center displacing the good leaving group, (X:)[51]

The sulfhydryl group, is the reactive function group in aprotin. at neutral pH, (N-ethylmaleimide, N-pyrenylmaleimide etc) reacts much faster with sulfhydryl groups than with amino groups (Figure2.28) . The resulting thioether bond is highly stable and can not be cleaved under physiological conditions [51]

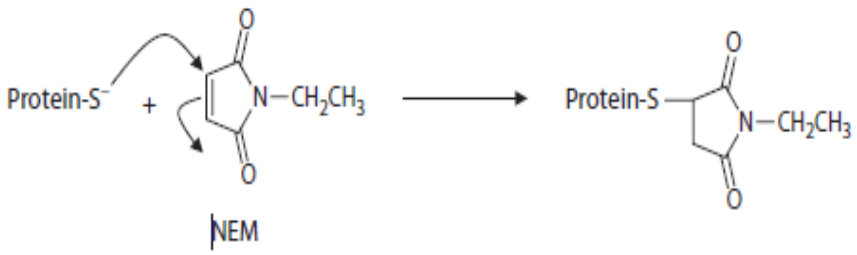

Figure 2.28 Reaction of N-ethylmaleimide (NEM) with sulfhydryl group [51]

The quantitative reaction of maleimides with thiol groups is important for the spectrophotometric quantitative determination of thiol groups. For example; The reduction in absorption at 300 nm of N-ethylmaleimide at a pH of 6 in a dilute solution can be used for the quantitative estimation of thiol groups. The abundance of the amino group in the protein domain makes it the most important chemical modification target. Compared to sulfhydryl groups, amino groups react very slowly and at high pH with α-Haloacetyl compounds. Even then, the reaction rate is only one-hundredth of that of the thiol. In proteins where there is no free sulfhydryl group or where the thiol is buried and unreactive, reactions that the amino groups give with α-Haloacetyl compounds become important. Like haloacetates Maleimide derivatives react only with amino groups at alkaline pH conditions. There are two conceivable ways in which amino groups can be react with maleimides (Figure 2.29). The amine nitrogen can attack the double bond of the maleimide ring or undergo acylation by addition to the carbonyl carbon group followed by ring opening. Whatever the reaction pathway, the reactions of maleimides with amines are important in the pH values above the neutral level [52] .

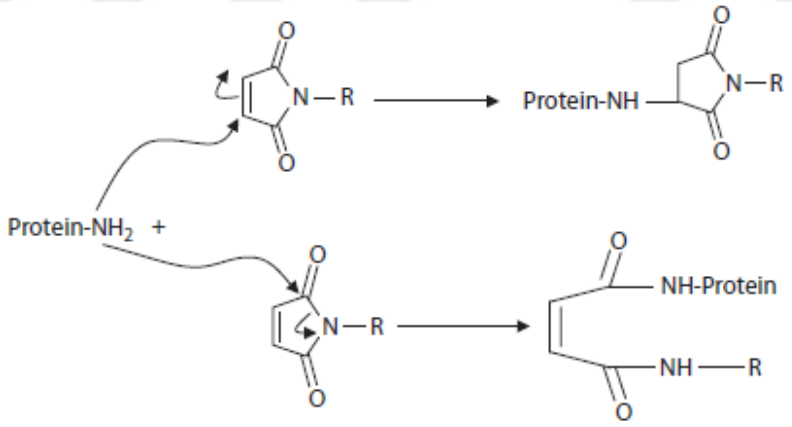

Figure 2.29 Reaction of N-maleimides with protein amino groups [52]

In Acylating agents the nucleophile attacks at the carbonyl carbon displacing a leaving group(Figure 2.30). Isocyanates and isothiocyanates react with amino, sulfhydryl, imidazolyl, thioxyl and carboxyl groups of proteins, but form stable products only with amino groups (Figure 2.30A&B) [51].

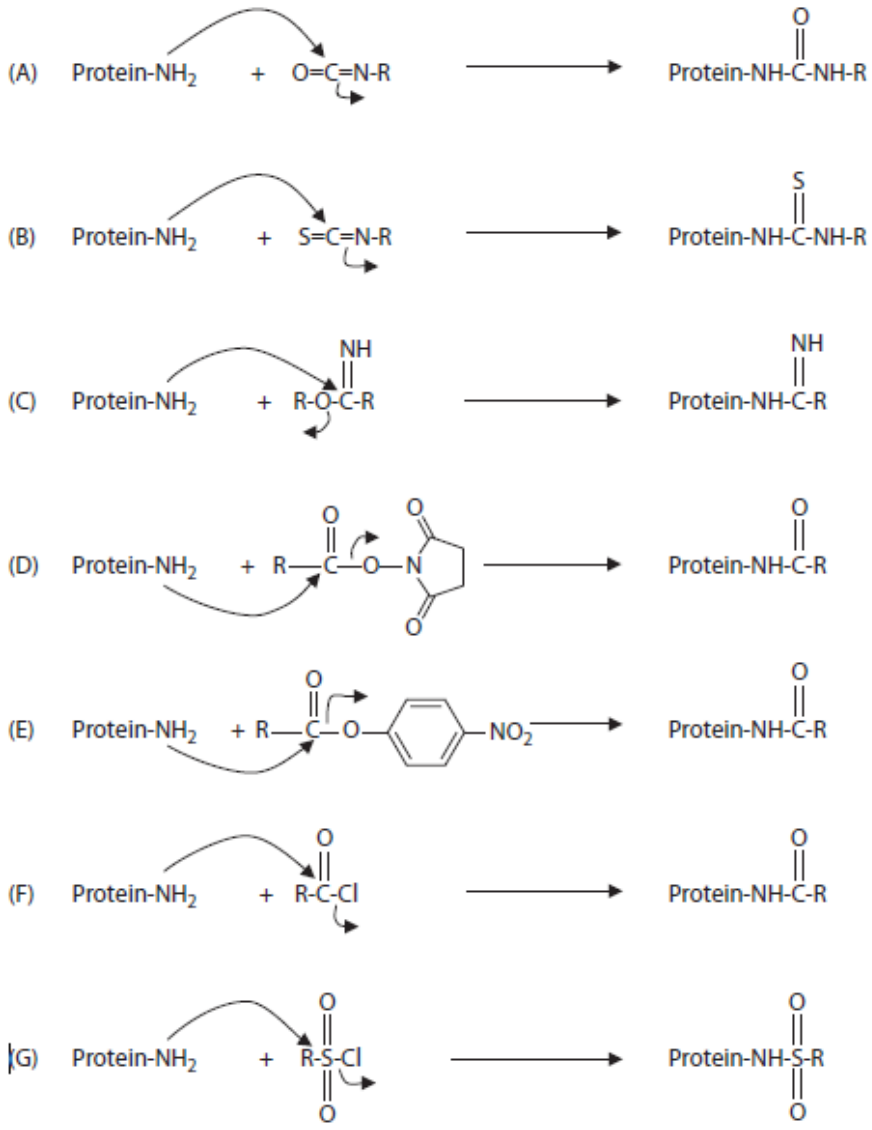

Figure 2.30 Acylation reactions of amino groups. Reaction with: (A) isocyanate; (B) isothiocyanate; (C) imidoesters; (D) N-hydroxysuccinimidyl ester; (E) p-nitrophenyl ester; (F) acyl chloride; and (G) sulfonyl chloride [52]

CHAPTER 3

MATERIALS AND METHODS

3.1 Chemical Materials and Devices Used

3.1.1 Chemical Materials Used

Material name	Company name	catalog No
Dimethyl sulphoxide (DMSO)	Fluka	34943
Bovine serum albumin (BSA)	Fluka	05488
$NaH_2PO_4 .2H_2O$	Fluka	71505
Sephadex G-75	Sigma	17-0050-01
Sodium chloride	Sigma	
Sodium hydroxide (NaOH)	Fluka	71689
Chymotrypsin	Fluka	27270
Poly(acrylic acid) (Mw=100000)	Merck	523925
1-Ethyl-3-(3-dimethylaminopropyl)carbodiimide (EDC)	Merck	800907
N- (1-Pyranyl) maleimide (PM)	Fluka	82656
Methyl alcohol	Merck	106008
Ethyl alcohol	Merck	818761
Chloroform	Merck	822265
Acetone	Merck	802912

3.1.2 Devices Used

- UV/Vis Spectrophotometer: UNICAM UV/Vis Spectrometer UV2 (YTÜ), cuvette Hellma, 104-QS (YTÜ).
- UV/Vis Spectrophotometer: 25 UV/Vis Spectrophotometer (YTÜ), cuvette Hellma, 104-QS (YTÜ).
- Distilled water device: Maxima Ultra-Pure Water (YTÜ).
- Analytical Balance: Sartorius ED224S (YTÜ).
- Time-resolved fluorescence spectrophotometer: PTI C-71 Time Master System (YTÜ), cuvette Hellma 111-QS (YTÜ), Hellma 119.000F-QS (YTÜ).
- Temperature controlled incubator with agitation: Sartorius Certomat IS (YTÜ).
- Gel Permeation Chromatography Device: Viscotek GPC max VE 2001 GPC Solvent/Sample Module. Kolon: Shimadzu Shim-Pack 300 diol (YTÜ).
- Ultracentrifuge: Sigma-3K30 (YTÜ).

3.2 The Purpose of Working, Scope and Applied Method

Proteolytic enzymes play essential role in many diseases; For example AIDS, cancer, SARS, etc., in addition to their physiological activities [7-9]. Cancer cells use proteases to destroy environmental tissues in order to open up areas of multiplication and spreading. Detection of different cancer cells and proteases produced by many harmful bacteria and viruses have great importance in diagnosing and preventing of contemporary diseases. Microanalysis methods have been developed to identify the activity of several protease species [9].

The most important problems encountered in monitoring the activities of proteolytic enzymes are the substrate selection and sensitivity of the applied assay [7]. Historically, hemoglobin and casein have been shown to be the most widely used substrates in proteolytic enzyme assays because they are inexpensive and readily available [7]. The natural substrates of proteases are usually complexed with an organic substance to form a structure which can produce specific signals that can be observed in the excitation or emission spectrophotometry systems. This process can also be applied to synthetic peptide substrates synthesized by considering the mechanism of action of the proteolytic

enzyme. The aim here is to display the characteristic changes of the signals as qualitative or quantitative responses to enzyme activity [7-9].

A large number of fluorescent organic molecules such as, Pyrene, Fluorescein, Rhodamine, Anthracene etc.- can be covalently attached to the functional groups (-COOH, -NH2, -OH, -SH) in the alkyl side chains of L-α-amino acids forming the proteins by applying appropriate chemical modifications. These complexes are synthesized for examination of proteins, monitoring of enzyme activity, permeability of membranes, clinical examinations and so on.

Conjugation with polymers to increase the catalytic stability of enzymes is an important research topic in the field of biomacromolecular chemistry, where detailed studies are still being carried out [1,51].

In our study, the differences between the proteolytic activities of free and conjugated forms of chymotrypsin enzyme with polyacrylic acid (PAA) on bovine serum albumin (BSA) were determined by time-resolved fluorometric method. For this purpose, PM-BSA complex was synthesized by binding "N-1-pyrenylmaleimide, (PM)" to BSA in the appropriate reaction conditions. The binding reaction was carried out in such a way as to form excimers which allowed us to observe sensitively the protease activity on PM-BSA.

N-1-pyrenylmaleimide (PM) is selectively attached to free sulfhydryl (-SH) groups at neutral pH, which is used for the quantitative determination of free-SH groups and hence cysteine amino acids in proteins [1,51]. BSA contains 35 cysteine amino acids and with the exception of the cysteine34 (Cys34), the others increase the stability of BSA by forming 17 disulfide bonds [53]. Accordingly, since the two pyrene rings need to be positioned face to face between the distances 0.3-0.5 nm in the appropriate locations in BSA structure to generate the excimer emission, the modification of the single free-SH group on Cys34 with PM in the BSA structure does not allow to produce excimer emissions. In this study, we used the binding ability of PM to both free "-SH" and free "-NH_2" groups in basic conditions (pH: 9) [51]. Excimer emissions which appeared as a new and widespread peak between 450-470 nm in the fluorescence spectra of Figures 4.11 and 4.14 proved that this modification has taken place on the amine groups. The changes in fluorescence lifetime distributions obtained by the exponential series method (ESM) analysis of the decay data of excimer emission was

used to determine the differences between free chymotrypsin and PAA-chymotrypsin activities.

In the literature, there is no study which explains the activity differences between free and PAA-conjugated chymotrypsin according to the changes in fluorescence lifetime distributions, which makes our thesis is unique.

CHAPTER 4

EXPERIMENTAL PART

The properties and application areas of biomacromolecules can be further expanded and improved by attaching synthetic polymers. Immobilization of enzymes has been taken to improve catalytic stability of enzymes and can expand the application of the neutral catalysts. there are many materials, including synthetic organic polymers, biopolymers, hydrogels, inorganic supports, and smart polymers, to be used to immobilize to enzyme, and good activity retention, and enhanced thermostability are often observed [1]. A range of functional groups which can be used in the covalent immobilization of enzymes include amino, hydroxyl, carboxyl and phenolic groups. The physical structure and chemical composition of support can also influence the microenvironment of the immobilized species and consequently their biological properties [2]. Conjugation and immobilization of enzymes with polymers may provide wide range industrial applications in medicine, diagnosis, life sciences, microelectronics and material sciences [3]. In this work we examined the activity of covalent conjugate of chymotrypsin with polyacrylic acid (PAA) on fluorescence lifetime distributions of PM-BSA complex by using time resolved spectrofluorometer. The aim of the study is to research whether if there were remarkable differences between the proteolytic effects of free chymotrypsin and PAA-conjugated chymotrypsin on the fluorescence lifetime distributions of PM-BSA complex. To determine this, we used the excimer fluorescence of PM-BSA synthesized according to the method of ref (54). The excimers are dimeric excited state complexes and maintain their presence only during the excitation time. When the excitation ceases, the dimeric state disappears. Detailed informations about the denaturation and hydrolysis of proteins can be obtained by using the excimer emission which can be easily affected by the changes in the three-dimensional structure of the protein [2,12-14,42,44,45].

The excited state dimers which are formed by the two same molecules are called excimers. The excited state dimers formed by the two different molecules are called exciplexes [2-5, 42, 45].

Our work was carried out by following a path as follows:

- Before PM-BSA synthesis, the fluorescence properties (fluorescence spectra, fluorescence decay curves, fluorescence lifetime distributions) of the reagents PM and BSA were determined in the time-resolved spectrofluorometer "PTI Time Master C 71".

- The PM-BSA complex was synthesised under appropriate reaction conditions (pH: 9, + 37 ° C), and the absorbance and fluorescence properties of the complex were determined.

- The synthesised complex PM-BSA was purified by gel filtration chromatography and by ultrafiltration.

- In the case of purified PM-BSA sample, the mole ratio "PM / BSA" was calculated.

- Conjugation of chymotrypsin enzyme with polyacrylic acid (PAA) was performed.

- The purified PM-BSA sample was exposed to the bioconjugate "PAA-chymotrypsin".

- Fluorescence spectra and fluorescence decay curves of the hydrolysate formed after the proteolysis were obtained from the time-resolved spectrofluorometer "PTI Time Master C 71". Fluorescence lifetime distributions were determined by exponential series method (ESM) analysis of the decay data, in Felix32 program installed in the computer of the spectrofluorometer.

- Fluorescence lifetime distributions of PM-BSA, and of PM-BSA hydrolysates produced by the activities of free and PAA-conjugated chymotrypsin were compared.

Fluorescence lifetime distribution produced from hydrolysate of PM-BSA by PAA-chymotrypsin bioconjugate showed that the activity of the chymotrypsin in the conjugate was significantly reduced. This result may be due to the covering of the active site of chymotrypsin with PAA as a result of covalent modification. However, even with an activity close to the end point, it was seen that the state of the peptides in the hydrolysate produced by PAA-conjugated chymotrypsin can be followed sensitively by changes in fluorescence lifetime distributions.

The steps of the work we have listed above are presented in details below:

4.1 Determination of Absorption and Emission Properties of N- (1-pyryl) maleimide (PM)

In order to determine the binding rates after PM-BSA synthesis, the molecular structure was determined from the "8 mg PM / ml DMSO" stock solution of PM shown in Figure (4.1). The absorbance spectrum of the $8x10^{-5}$ M solution prepared in the Tris.HCl buffer (0.025 M, 0.1 M NaCl, 0.005 M $CaCl_2$, pH: 8) was taken using the Hellma 104-QS quartz cuvette in a "Perkin Elmer Lambda 25 UV / Vis Spectrophotometer" (Figure 4.2).

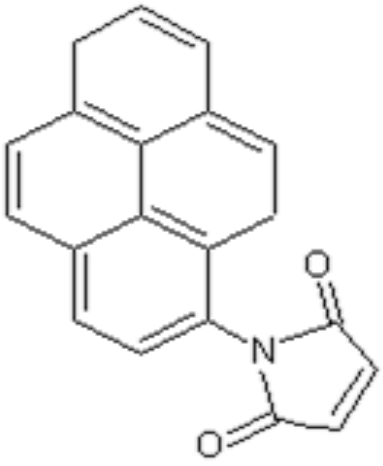

Figure 4.1 N- (1-pyrenyl)maleimide (PM)

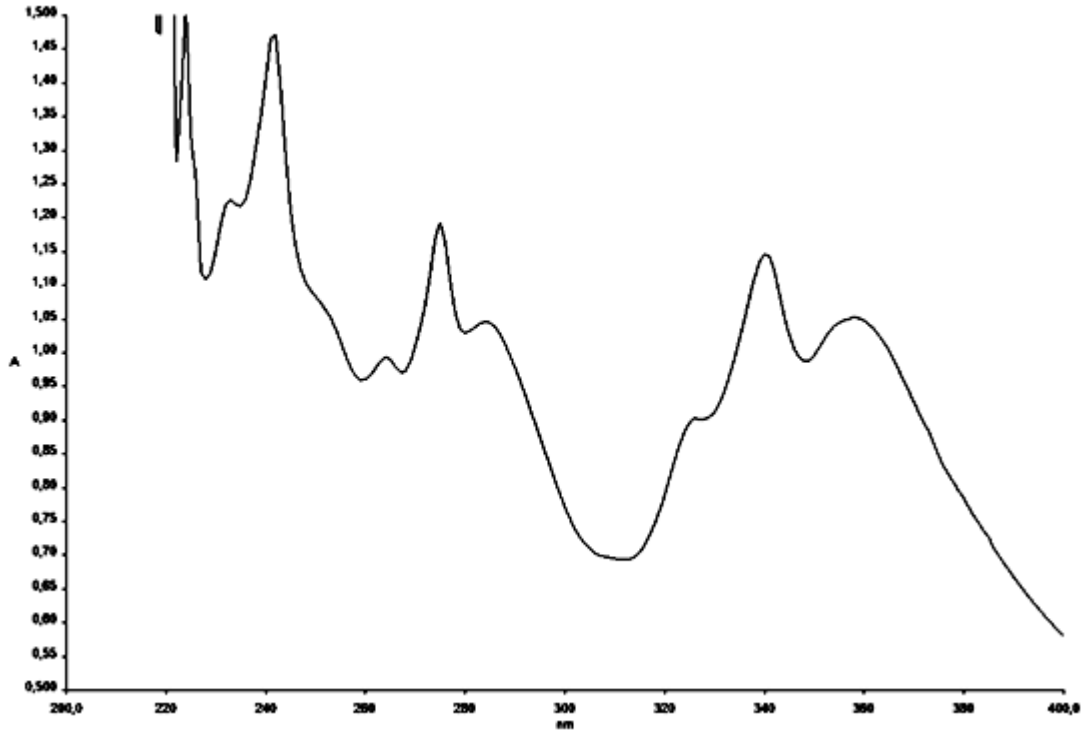

Figure 4.2 The absorbance spectrum of $8x10^{-5}$M PM A_{280} = 1.0291; A_{344} = 1,0548; Blank: 1.994 ml Tris.HCl (pH: 8) and 6 µl DMSO (0.3%) mixture prepared in Tris.HCl buffer (0.025M, 0.1M NaCl, 0, 005M $CaCl_2$, pH: 8)

Figure 4.2 shows the absorbance of PM at 280 nm this absorbance coincides with the characteristic absorbance of PM-BSA at 280 nm due to the protein content (Figure 4.8). The contribution of PM absorbance to PM-BSA absorbance was corrected using correction factor (CF = $A_{PM\text{-}280nm}$/ $A_{PM\text{-}344nm}$ = 1.0291/1.0548 = 0,976).

The time-resolved fluorescence spectrum of PM was taken under the same conditions (Figure 4.3).

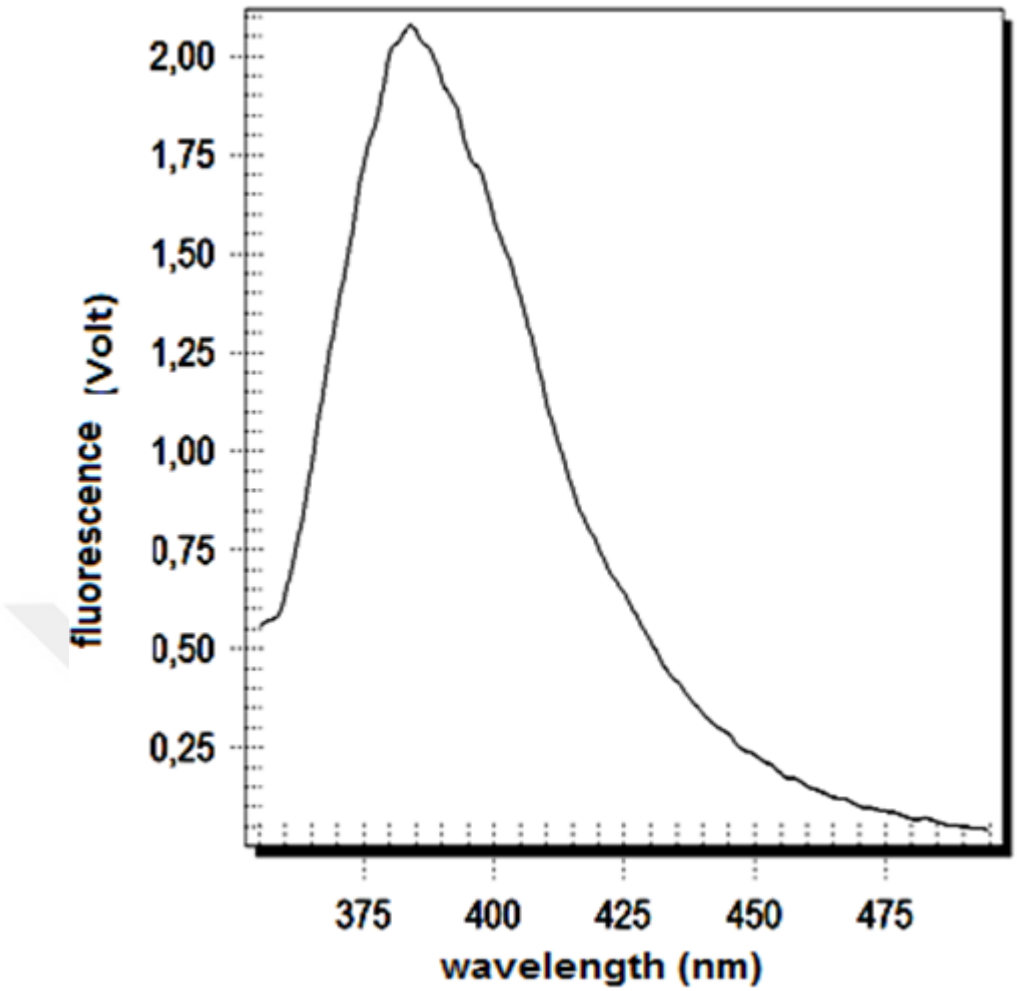

Figure 4.3 Time-resolved fluorescence spectrum of $5x10^{-5}$M PM in Tris.HCl buffer (0,025M, 0,1M NaCl, 0,005M $CaCl_2$, pH: 8). λ_{exc}: 337nm; $\lambda_{emis\text{-}max\text{-}monomer}$: 382nm; Integration time : 0,1 s; step size: 0,25; delay time: 117 ns; averages: 3

As seen in Figure 4.3, the characteristic monomer emission peak of PM was observed around 382 nm. The fluorescence decay of PM by time at the wavelength 382 nm is shown in Figure 4.4.

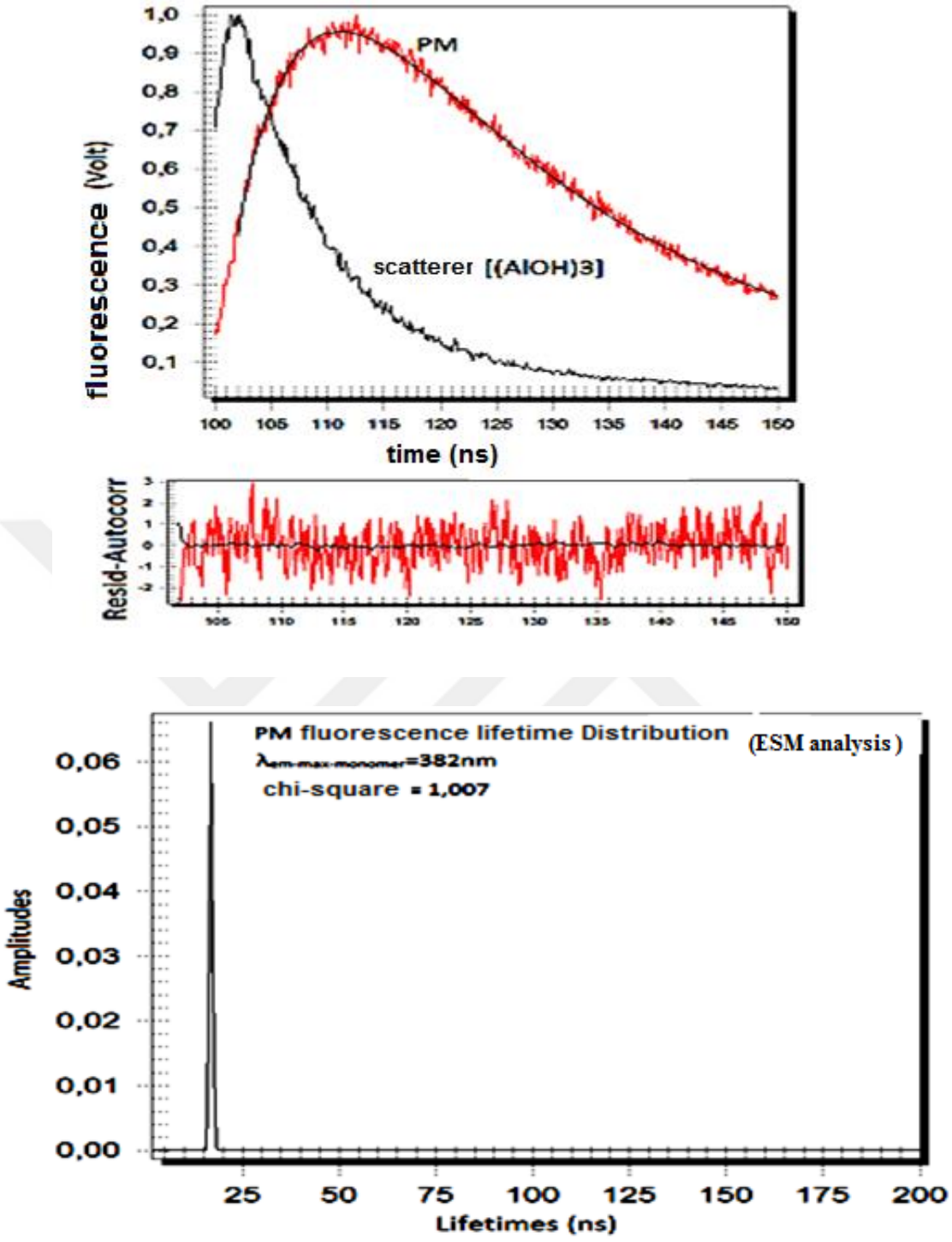

Figure 4.4 Fluorescence decay curve of 3×10^{-5} M PM in Tris.HCl buffer (0.025M, 0.1M NaCl, 0.005M $CaCl_2$, pH: 8), fitting curve of the decay data and fluorescence lifetime distribution (ESM, Chi-square: 1.007). Scattering curve shows a profile of lamp pulse reduction over time. λ_{exc}: 337 nm; $\lambda_{emisi.max}$: 382 nm; Integration time: 0,1; Channels: 400; averages: 3

ESM analysis procedure, embedded in Felix32 program installed in the computer of the spectrofluorometer, is applied to fluorescence decay data of PM. Fitting of the decay data, which was described as exponential series, to a curve was acquired by applying chi-square analysis (Equation 2.43) and thus the obtained data of the fitted curve was used to draw the lifetime distribution. The chi-square value of PM was calculated as 1,007. The fluorescence lifetime distribution of PM is between 15-20 ns and it is seen in Figure 4.4.

4.2 Absorption and Emission Properties of BSA

The three amino acids containing rings (tryptophan, tyrosine, phenylalanine) are responsible for light absorption in proteins, giving a maximum in UV region at 280 nm as shown in the spectrum of BSA in Tris.HCl buffer (pH: 8) (Figure 4.5). The absorption of tryptophan is about four times higher than that of tyrosine under certain conditions and at equal concentrations.

Fluorescence character of tryptophan is also dominant to the other two amino acids'. Tryptophan-derived protein fluorescence varies depending on the environmental conditions of the location of tryptophan in the protein structure. Conformational changes, interactions of subunits, substrate binding and denaturation are the major factors affecting the environmental conditions in which tryptophan is present.

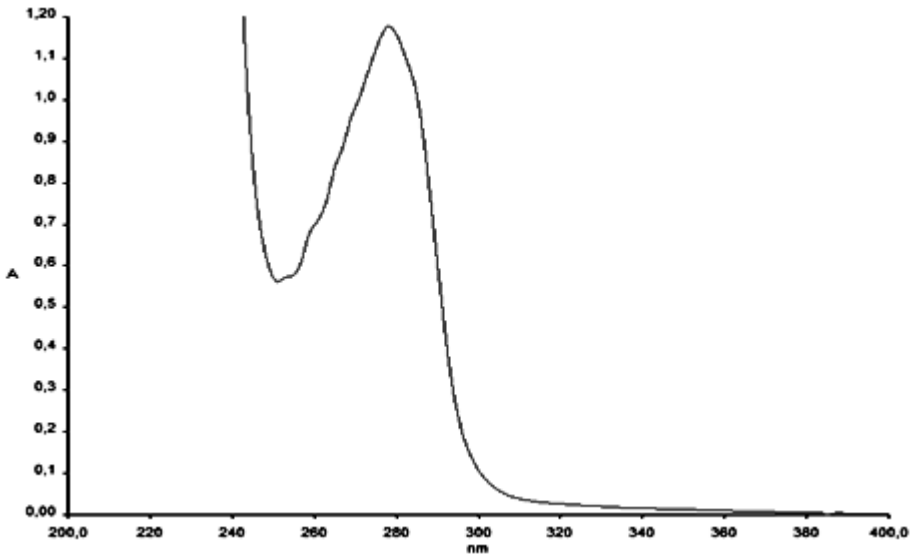

Figure 4.5 Absorbance spectrum of $3x10^{-5}$ M BSA in Tris.HCl buffer (0.025 M, 0.1 M NaCl, 0.005 M $CaCl_2$, pH: 8)

The fluorescence spectrum of BSA taken under the same conditions as PM is shown in Figure 4.6 .

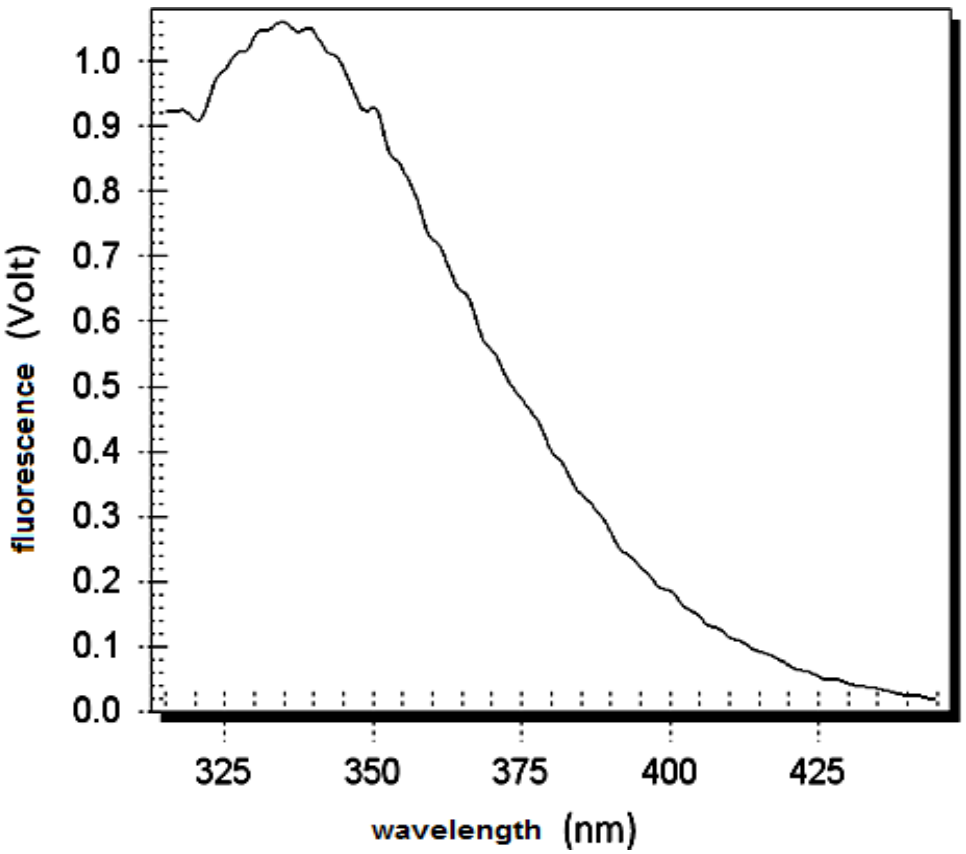

Figure 4.6 Time- resolved fluorescence spectrum of $8x10^{-5}$ M BSA in Tris.HCl buffer (0.025 M, 0.1 M NaCl, 0.005 M $CaCl_2$, pH: 8). λ_{exc}: 295 nm; $\lambda_{emis.max}$: 334 nm; Integration time : 0,1; Step size: 0.25; Delay time: 117ns; averages: 3

The maximum fluorescence emission of BSA is observed around 334 nm in the time-resolved fluorescence spectrum in Tris.HCl buffer (0.025M, 0.1M NaCl, 0.005M CaCl2, pH: 8) (Figure 4.6). By using ESM analysis procedure included in the Felix 32 program, the fluorescence lifetime distribution of BSA was obtained from the best fitted curve of fluorescence decay data described as exponential series, by applying chi-square analysis (Equation 2.46) and the chi-square value was calculated as 0.9949 (Figure 4.7). It is shown in Figure 4.7 that the fluorescence lifetime variation of BSA is distributed in the form of two peaks at around 4 ns and 6 ns.

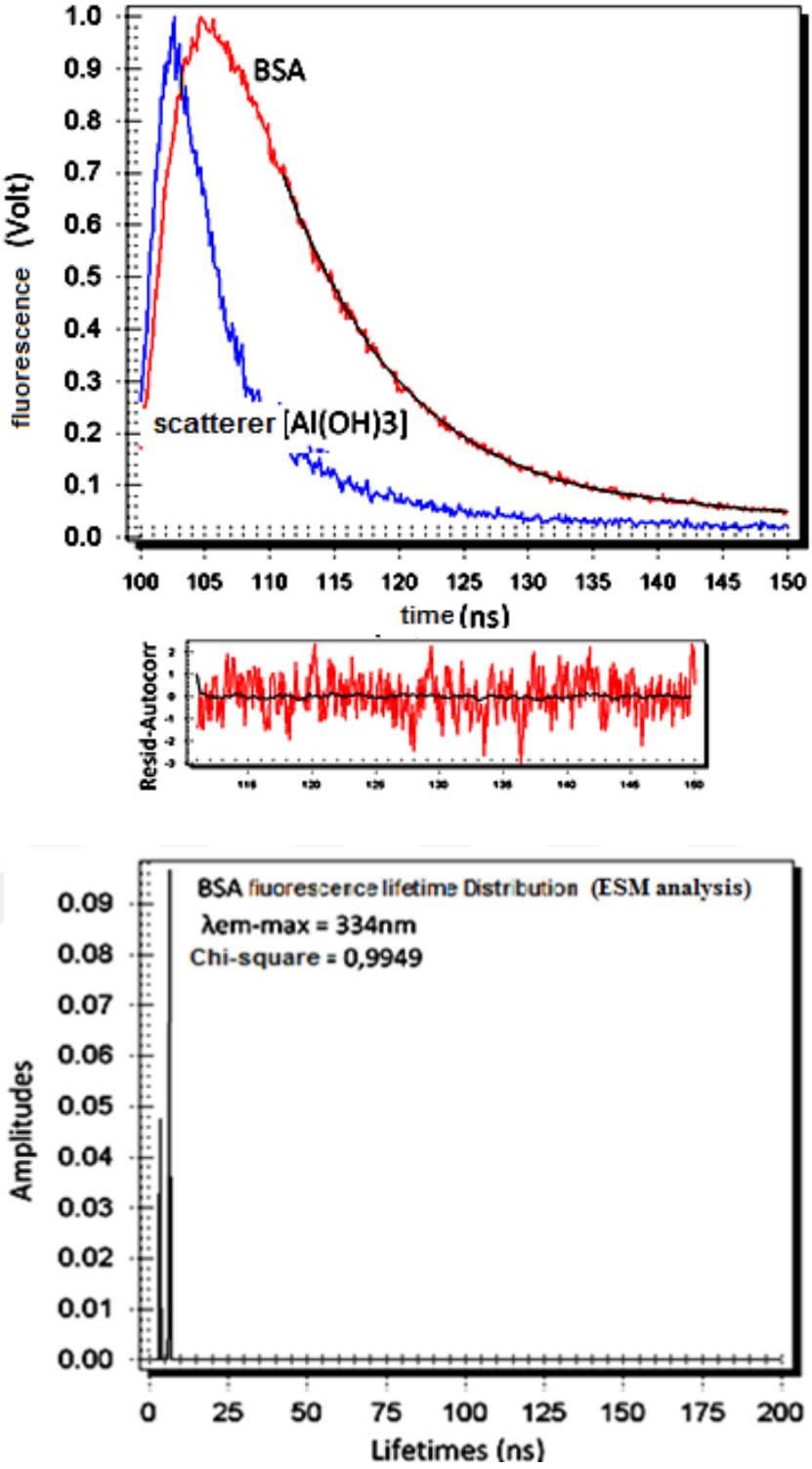

Figure 4.7 Fluorescence decay curve of $8x10^{-5}$ M BSA in Tris.HCl buffer (0.025 M, 0.1 M NaCl, 0.005 M $CaCl_2$, pH: 8), fitting curve of the decay data and fluorescence lifetime distribution (ESM, Chi-square: 0.9949). Scattering curve shows the change in lamp pulses over time. λ_{exc}: 295 nm; $\lambda_{emis.max}$ 334 nm; Integration time: 0,1; Channels: 400; averages: 3

4.3 Synthesis of PM-BSA complex

The amount of protein used in the modification reactions of fluorescent substance proteins is usually "1 mg Protein / ml" or more [14,44,55]. In this study in order to generate excimer fluorescence, "**20 mg BSA / ml**" BSA stock solution was prepared in phosphate buffer [PBS] (PBS; 0.01 M NaH2PO4, 0,15 M NaCl, pH: 9), which will provide the maximum amount of PM binding to the free -SH and $-NH_2$ groups of BSA[56]. PM stock solution was prepared in dimethylsulfoxide (DMSO) at a concentration of "**8mg.PM / ml.DMSO"** and stored at + 4 °C for extended periods of use.

For the conjugation reaction of BSA with PM, in an Eppendorf tube of 1000µL;

I. 250 µl. "20 mg.BSA / ml PBS" BSA stock solution,

$$n_{BSA} = \frac{m_{BSA}}{MW_{BSA}} = \frac{20\times10^{-3}(g)\times\dfrac{250\mu l}{1000\mu l}}{66000} \cong 7{,}58\times10^{-8} mol \text{ BSA/250µl PBS} \qquad (4.1)$$

II. 282 µl. "8 mg.PM/ml DMSO" PM stock solution, (MW_{pm} = 297.32)

PM mole ratio 100 times more than BSA. The aim of this molar excess selection is to modify the free ε-NH2 groups of sixty lysine amino acids of BSA with PM as high as possible, besides the single free -SH group of cysteine-34 amino acid of BSA. For this purpose, the volume to be taken from PM stock solution was calculated. According to this, to get "$n_{PM} = n_{BSA}\times100 = 7{,}58\times10^{-8}\times100 = 7{,}58\times10^{-6} mol$" PM, The volume to be taken from PM stock solution is;

$$V = \frac{7{,}58\times10^{-6}\times1000\mu l.(DMSO)}{\dfrac{8\times10^{-3}(g)PM}{297{,}32}} = 281{,}7107\mu l \cong 282\mu l. \text{"Stock PM"} \qquad (4.2)$$

and

III. 468 µl PBS buffer (0,01M NaH_2PO_4, 0,15M NaCl, pH: 9)

mixed and the reaction mixture was allowed to react at + 37 ° C for 24 hours in a shaking incubator.

4.4 Purification of PM-BSA

To separate the PM-BSA complex from the reaction mixture, a separation column (the sizes of filling; 1.5x20 cm) filled with Sephadex G-75 gel was used. Bidistilled water was applied to the column as mobile phase and the fractions were collected in tubes (2 ml). The fractions containing PM-BSA were determined at 344 nm by using UV / Vis spectrophotometer and were combined in a volume of 6 ml in a concentrator "Vivaspin 6 Centrifugal Concentrator" (Sartorius Stedim Biotech GmbH, Vivaproducts) and were centrifuged in "SIGMA 3K30" refrigerated centrifuge at 10,000 rpm for 2 h at + 4 °C. The obtained pure PM-BSA sample was dissolved in a buffer of Tris.HCl (0.025M, 0.1M NaCl, 0, 005M CaCl2, pH: 8) suitable for hydrolysis with PAA-chymotrypsin to prepare 6ml PM-BSA stock solution. The mole ratio calculations performed by using the method in ref. 57 revealed that one BSA molecule binds 6 PM molecules.

4.5 Calculation of PM / BSA Mole Ratio in PM-BSA Complex

1 ml of the PM-BSA stock solution obtained at the end of the purification was taken and diluted to 3 ml with Tris.HCl buffer (0.025M, 0.1M NaCl, 0, 005M CaCl2, pH: 8). This diluted solution was analyzed by UV / Vis spectrophotometer, $A_{PM\text{-}BSA(280nm)}$=0,64939 and A_{344nm}=0,47672 Absorbance values (Figure 4.8).

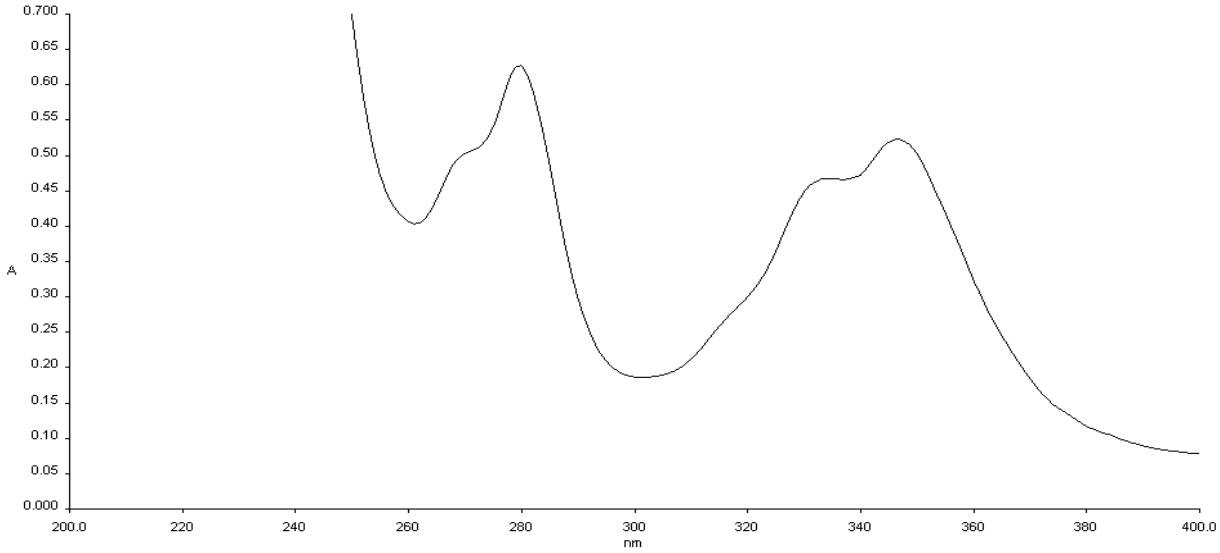

Figure 4.8 Absorbance Spectra of PM-BSA complex in Tris.HCl buffer (0.025M, 0.1M NaCl, 0.005M $CaCl_2$, pH: 8). $A_{PM\text{-}BSA(280nm)}$ = 0,64939; $A_{PM(344nm)}$=0,47672; Blank: Tris.HCl (pH: 8).

In Equation 2.30 The concentration of the Lambert-Beer law in terms of absorption,

$$C = \frac{A}{\varepsilon \times b} \tag{4.3}$$

If we rate the concentrations of PM and BSA in the PM-BSA complex, We can write equality as follows:

$$\frac{C_{PM}}{C_{BSA}} = \frac{\frac{n_{PM}}{V(l)}}{\frac{n_{BSA}}{V(l)}} = \frac{\frac{A_{PM(344nm)}}{\varepsilon_{PM(344nm)\times b}}}{\frac{A_{BSA(280nm)}}{\varepsilon_{BSA(280nm)\times b}}} \tag{4.4}$$

Since the volumes (V) and the path of the light (b = 1cm) in the tub are the same, this expression can be simplified as shown in equation 4.5.

$$\frac{C_{PM}}{C_{BSA}} = \frac{\frac{n_{PM}}{V(l)}}{\frac{n_{BSA}}{V(l)}} = \frac{\frac{A_{PM(344nm)}}{\varepsilon_{PM(344nm)}}}{\frac{A_{BSA(280nm)}}{\varepsilon_{BSA(280nm)}}} \tag{4.5}$$

Figure 4.2 shows that PM has an absorbance at 280nm. In this case, the absorption observed at 280 nm of the PM-BSA complex equals the sum of the absorptions given in equation 4.6.

$$A_{PM-BSA(280nm)} = A_{BSA(280nm)} + A_{PM(280nm)} \tag{4.6}$$

If we leave alone the absorption of BSA in the equation 4.6, we get the equation 4.7.

$$A_{BSA(280nm)} = A_{PM-BSA(280nm)} - A_{PM(280nm)} \tag{4.7}$$

In order to determine the absorbance contribution of PM ($A_{PM(280nm)}$) in the PM-BSA complex, we can use the absorbance value of pure PM assuming that the BSA absorption does not change with the complex formation [57]. The absorbance values of the $8x10^{-5}$M PM in the Tris.HCl buffer (pH: 8) at 280 nm and 344 nm in Fig. 4.2 are A_{280}=1,0291and A_{344}=1,0548, respectively. When these absorbance values of pure PM are rated to each other, we get a constant as a correction factor (CF) in the equation 4.8;

$$\frac{A_{PM\,(280nm)}}{A_{PM\,(344nm)}} = \frac{1{,}0291}{1{,}0548} = 0{,}9756351915 \cong 0{,}976 \tag{4.8}$$

and by using the correction factor (CF) from equation 4.8, we can express the absorbance of PM at 280 nm in terms of the absorbance at 344 nm as seen in equation 4.9,

$$A_{PM\,(280nm)} = 0{,}976 \times A_{PM\,(344nm)} \tag{4.9}$$

and accordingly we can rewrite the equation 4.7 as follows (equation 4.10);

$$A_{BSA(280nm)} = A_{PM-BSA(280nm)} - 0{,}976 \times A_{PM\,(344nm)} \tag{4.10}$$

and by using the equation 4.10 which expresses the pure BSA absorbance in the PM-BSA complex, we can rewrite the equation 4.5 too as in equaiton 4.11, which expresses the mole ratios of PM and BSA in the PM-BSA complex as follows.

$$\frac{C_{PM}}{C_{BSA}} = \frac{n_{PM}}{n_{BSA}} = \frac{\dfrac{A_{PM\,(344nm)}}{\varepsilon_{PM\,(344nm)}}}{\dfrac{A_{PM-BSA(280nm)} - 0{,}976 \times A_{PM\,(344)}}{\varepsilon_{BSA(280nm)}}} \tag{4.11}$$

Equality is reached.

After this stage, the molar absorptivities must be determined. Standard absorption curves prepared for BSA and PM were used for this purpose (Table 4.1, Figure 4.9 and Table 4.2, Figure 4.10).

Table 4.1 Absorbance values of BS at 280nm according to concentration

C_{BSA}(Molar)	A_{280}
$1x10^{-6}$	0.037
$3x10^{-6}$	0.128
$5x10^{-6}$	0.199
$8x10^{-6}$	0.307
$1x10^{-5}$	0.354

For BSA, absorbance values corresponding to the concentrations in (Table 4.1) were plotted using the program "OriginPro7.0" and linear regression was applied (Figure 4.9). The slope value of the curve obtained with R = 0,99573 reliability level, m = 37246,23116 was found. This slope value was taken as molar absorptivity ($\varepsilon_{BSA(280nm)}$) for BSA.

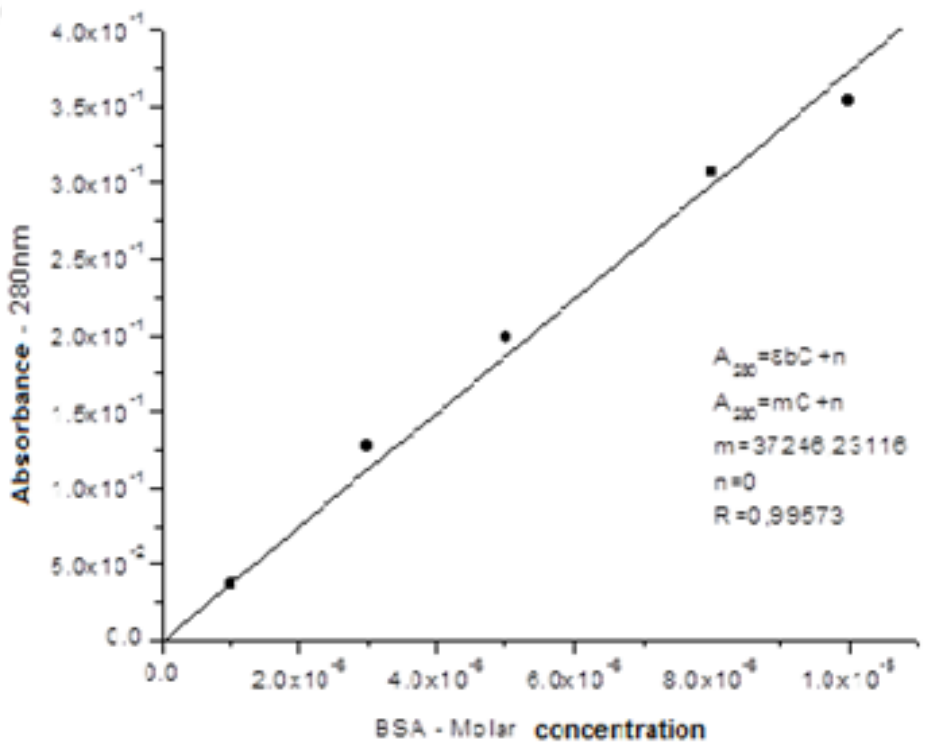

Figure 4.9 Absorbance standard curve of BSA in Tris.HCl buffer (0,025M, 0,1M NaCl, 0,005M $CaCl_2$, pH: 8)

To determine the molar absorptivity of PM, the absorbance values corresponding to the concentrations in Table 4.2 were plotted using the program "OriginPro 7.0" and linear regression was applied (Figure 4.10).

Table 4.2Absorbance values of PM according to concentration at 344nm

C_{PM}(Molar)	A_{344}
$1x10^{-6}$	0,021
$3x10^{-6}$	0,048
$5x10^{-6}$	0,090
$8x10^{-6}$	0,138
$1x10^{-5}$	0,149

The slope value of the curve obtained with reliability level R = 0.98943 is m = 16125,62814. The obtained slope value was taken as molar absorptivity for PM ($\varepsilon_{PM(344nm)}$).

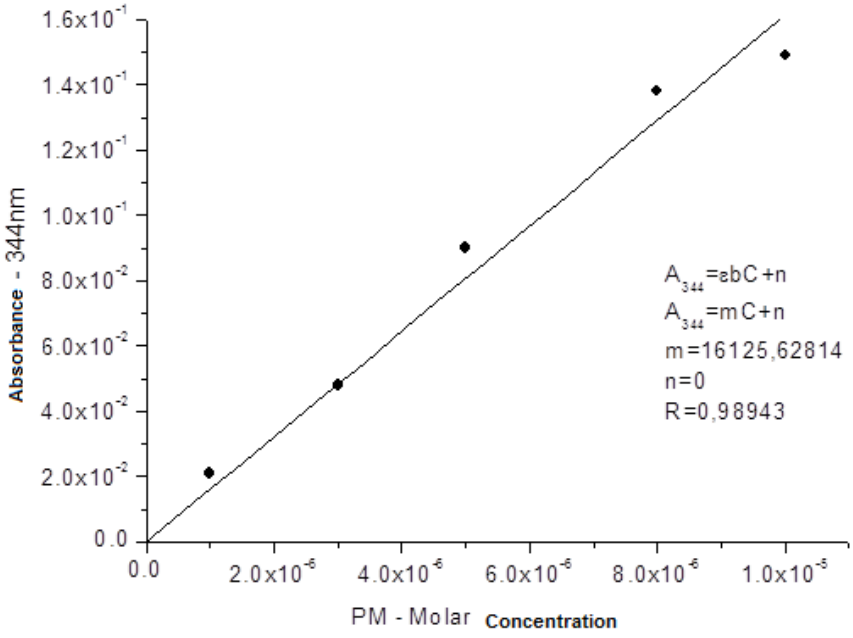

Figure 4.10 Absorbance standard curve of PM in Tris.HCl buffer (0,025M, 0,1M NaCl, 0,005M $CaCl_2$, pH: 8)

When the molar absorptivities of PM and BSA calculated from the standard curves are placed in equation 4.11, the equation 4.12 is obtained.

$$\frac{C_{PM}}{C_{BSA}} = \frac{n_{PM}}{n_{BSA}} = \frac{\frac{A_{PM\,(344nm)}}{16125,62814}}{\frac{A_{PM-BSA(280nm)} - 0,976 \times A_{PM\,(344)}}{37246,23116}} \qquad (4.12)$$

When the absorbance values of PM-BSA complex at 280 nm and 344 nm are placed in equation 4.12, the molar ratio "n_{PM}/ n_{BSA}" in the PM-BSA complex is found to be 6 (Equation 4.13).

$$\frac{C_{PM}}{C_{BSA}} = \frac{\frac{0,47672}{16125,62814}}{\frac{0,64939 - 0,976 \times 0,47672}{37246,23116}} = \frac{2,95628794 \times 10^{-5}}{4,943084824 \times 10^{-6}} = 5,980653874 \cong 6 \qquad (4.13)$$

4.6 Fluorescence Properties of PM-BSA complex

Since the phosphate buffer inhibits the proteases, it was only used for the binding reaction of PM to BSA and the hydrolysis reaction of PM-BSA with the protease chymotrypsin was carried out by using Tris.HCl buffer [12].

Before treatment PM-BSA with chymotrypsin, the time-resolved fluorescence spectrum (Figure 4.11), fluorescence decay graph and fluorescence lifetime distribution (Figure 4.12) of PM-BSA complex were obtained in Tris.HCl buffer with pH=8 for optimum activity of chymotrypsin.

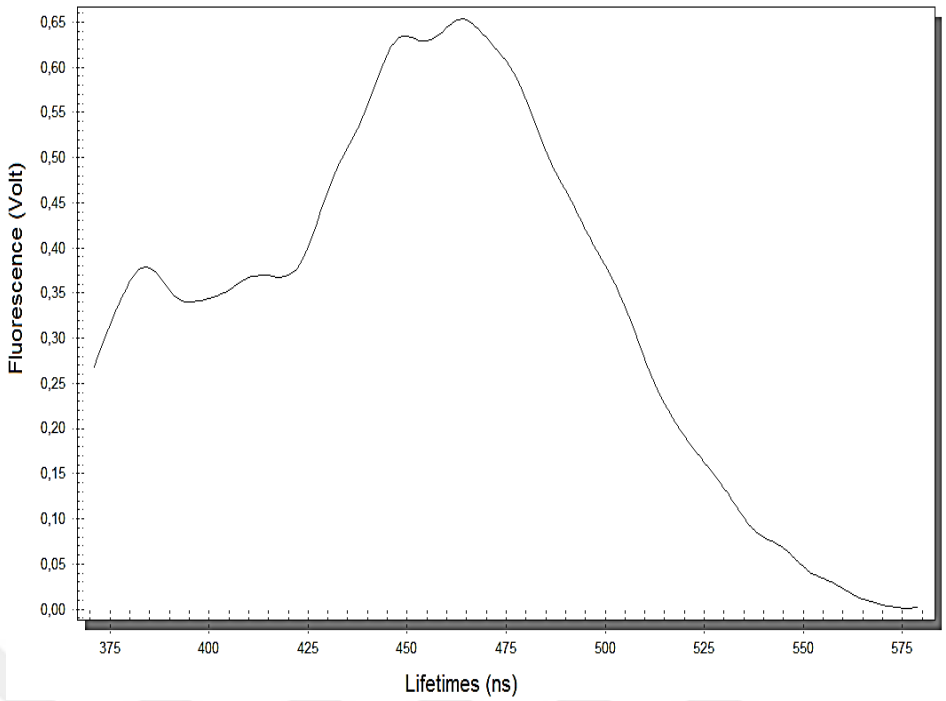

Figure 4.11 Time-resolved fluorescence spectrum of PM-BSA solution in Tris.HCl buffer (0.025M, 0.1M NaCl, 0.005M $CaCl_2$, pH: 8). λ_{exc}: 337nm; $\lambda_{emis.max}$: 384 nm (monomer); $\lambda_{emis.max}$: 464 nm (excimer); Integration Time : 0,1; Step size: 0.25nm; Delay time: 60ns; averages:3

In Figure 4.11, the fluorescence spectrum of PM-BSA shows the excimer emission as a new and widespread peak at about 464 nm, which indicates that two PM molecules are positioned at a distance of 0.3 nm or closer on BSA [42,44,45]. It means that maleimide which binds only free thiol (sulfhydryl) groups at neutral pH was also bounded to free amine groups at basic pH. The changes of the fluorescence lifetime distribution of excimer emission (Figure 4.12) by the effect of chymotrypsin is specific to chymotrypsin activity.

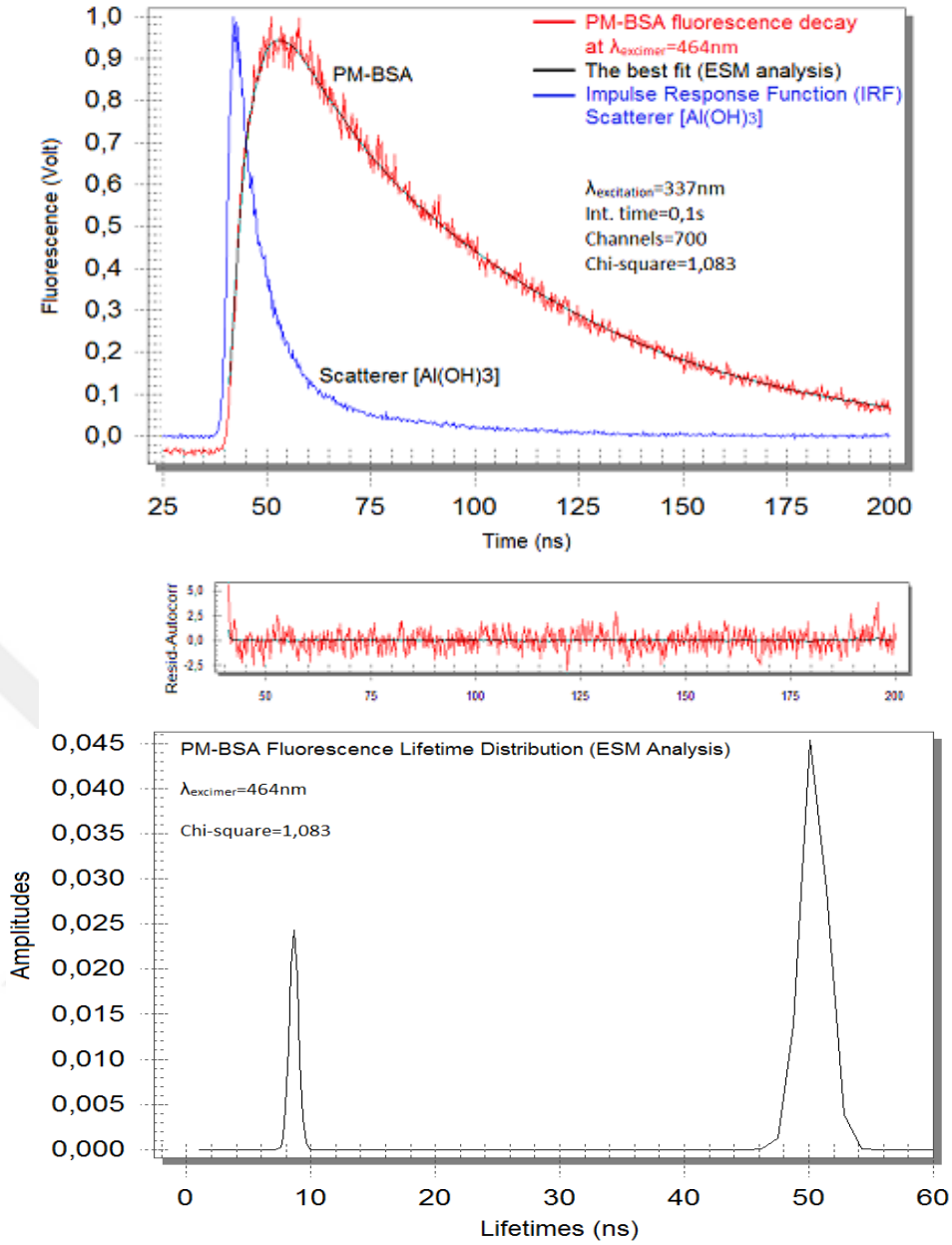

Figure 4.12 Fluorescence decay curve of PM-BSA solution in Tris.HCl buffer (0,025M, 0,1M NaCl, 0,005M $CaCl_2$, pH: 8), fitting curve of the decay data and fluorescence lifetime distribution (ESM, Chi-square: 1.083). Scattering curve shows the change in lamp pulses over time. λ_{exc}: 337 nm; $\lambda_{excimer.max}$: 464 nm; Integration time : 0,1; Channels: 700; averages: 3

Figure 4.12 shows the fluorescence decay curve of excimer emission of PM-BSA at $\lambda_{excimer.max}$: 464nm, the best fit curve of the decay data, and the fluorescence lifetime distribution. it is seen that excimer species with longer-lifetimes are collected around 50 ns and excimer species with shorter-lifetimes are collected around 7-9 ns.

The fluorescence lifetime distribution of the PM-BSA complex shows that the complex structure of the PM and BSA molecules differs in the range of 48-53 ns when compared to the fluorescence lifetime distributions (Figure 4.4, Figure 4.7), resulting in longer lifetime fluorescence emission systems. This difference in distribution, which is observed in the fluorescence lifetimes resulting from excimers located in different regions of BSA, is specific to the PM-BSA complex. In this study, it was determined that the distribution obtained by the hydrolysis of free chymotrypsin was significantly different from the distribution obtained by the hydrolysis of the PAA-chymotrypsin conjugation complex.

4.7 Synthesis of PAA-Chymotrypsin

The ratio of PAA-chymotrypsin polymer-enzyme conjugate was 1: 1 [58]. For this purpose, 1 ml of $2{,}7615 \times 10^{-3}$M PAA stock solution (d=0,789g/ml; %35; Mw=100000) was taken and diluted to 10 ml with TrisHCl buffer (pH: 5). 0,5523g of 1-ethyl-3- (3-dimethylaminopropyl) carbodiimide (EDC, MW = 191,7) was added to the diluted solution of $2{,}7615 \times 10^{-4}$M PAA and the mixture was incubated on a magnetic stirrer for activation along 2 hours, and after that 1 ml of 0.0012M chymotrypsin solution is added and the last mixture was left to incubation at room temperature for 12 hours to obtain PAA-chymotrypsin bioconjugate. The bioconjugate concentration was calculated as $M_{PAA\text{-}chymotrypsin}=6{,}93815 \times 10^{-5}$M using absorbance (($A_{280(PAA\text{-}chymotrypsin)}=2{,}5842$)) and molar absorptivity ($\varepsilon=37246{,}23116$) measured at 280 nm in UV-VIS spectrophotometer. The proteolytic effects of PAA-chymotrypsin conjugate on PM-BSA complex were investigated by UV-VIS spectrophotometer and time-resolved spectrofluorimetry techniques.

4.8 Investigation of PAA-Chymotrypsin Conjugation Effect on PM-BSA Complex by UV-VIS Spectrophotometer

100, 200, 300, 400, 500 µl samples from stock PM-BSA ($4{,}94 \times 10^{-6}$M, pH = 8, TrisHCl, equality 4.13) were diluted to 2 ml with Tris.HCl buffer (pH: 8) and thus $2{,}47 \times 10^{-7}$, $4{,}94 \times 10^{-7}$, $7{,}41 \times 10^{-7}$, $9{,}88 \times 10^{-7}$, $1{,}235 \times 10^{-6}$ molar concentrations PM-BSA were prepared. The average of the differences between the absorbance values taken over 5 minutes with the intervals of 30 seconds in UV-VIS spectrophotometer by adding 36 µl of $6{,}93815 \times 10^{-5}$M PAA-Chymotrypsin ($1{,}235 \times 10^{-6}$M, 2ml) conjugate into each solution

and Lineweaver-Burk graph was drawn in the excel program using the concentration and absorbance values at 344nm.

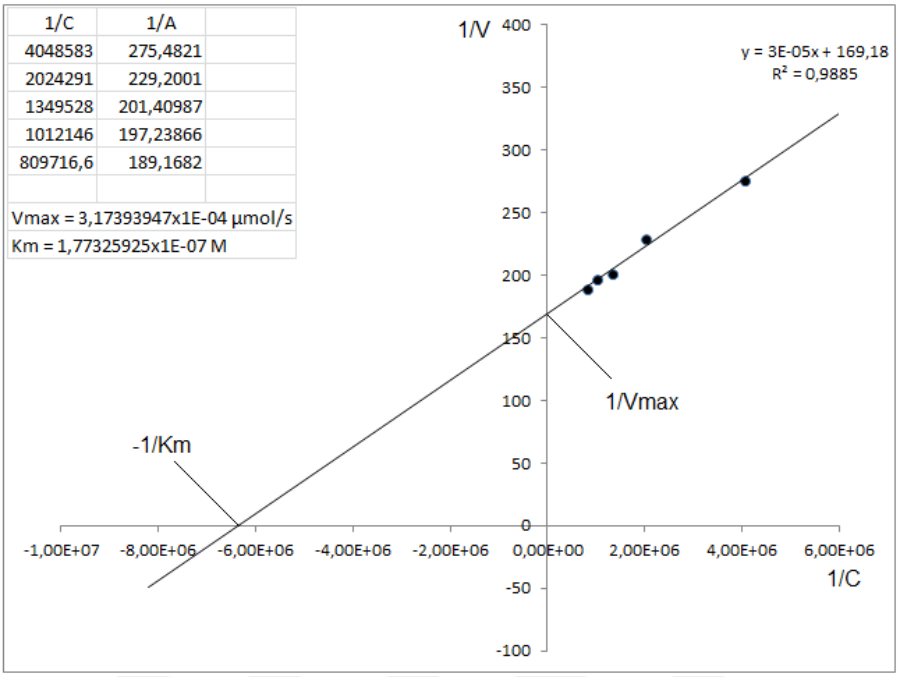

Figure 4.13 Lineweaver-Burk graph obtained from the hydrolysis of PM-BSA complex by PAA-chymotrypsin conjugate

Using the graphical equation ($y = 3x10^{-5}x + 169,18$; $R^2=0,9885$), Vmax and Km were found as $Vmax=3,174x10^{-4}$µmol/s and $Km=1,77326x10^{-7}$M. These results show that there is a large decrease in Km and Vmax values [59]. Accordingly, the conjugation of chymotrypsin with PAA by covalent modification caused a significant loss of activity.

4.9 Investigation of PAA-Chymotrypsin Conjugation Effect on PM-BSA Complex by Time-resolved Spectrophotometer

The concentration of PM-BSA stock solution (pH = 8, TrisHCl) was calculated to be $4,94 \times 10^{-6}$M by using absorption values of this solution given in (Figure 4.8) $A_{PM\text{-}BSA(280nm)}$= 0,64939; $A_{PM(344nm)}$=0,47672,), the molar absorption value $\varepsilon_{BSA(280nm)}$=37246,23116 obtained from the BSA standard absorption curve (Figure 4.9) in the portion of the equilibrium 4.12 corresponding to C_{BSA}. 500 µl of the PM-BSA stock solution (pH = 8, TrisHCl) was taken and diluted to 2 ml with Tris.HCl buffer (pH: 8) ($M_{PM\text{-}BSA(0,5)}=1,235x10^{-6}$M). Into this solution, 36 µl of PAA-chymotrypsin

conjugate ($M_{PAA\text{-}chymotrypsin}$=6,93815x10^{-5}M) was added providing the molar ratio ($n_{PM\text{-}BSA}/n_{PAA\text{-}chymotrypsin}$)=1 for complete hydrolysis of the PM-BSA complex, and left in water bath for 24 hours at 30 °C. Fluorescence changes of the PM-BSA by the activity of PAA-chymotrypsin conjugate were obtained and compared with the fluorescence changes under free chymotrypsin effect [57].

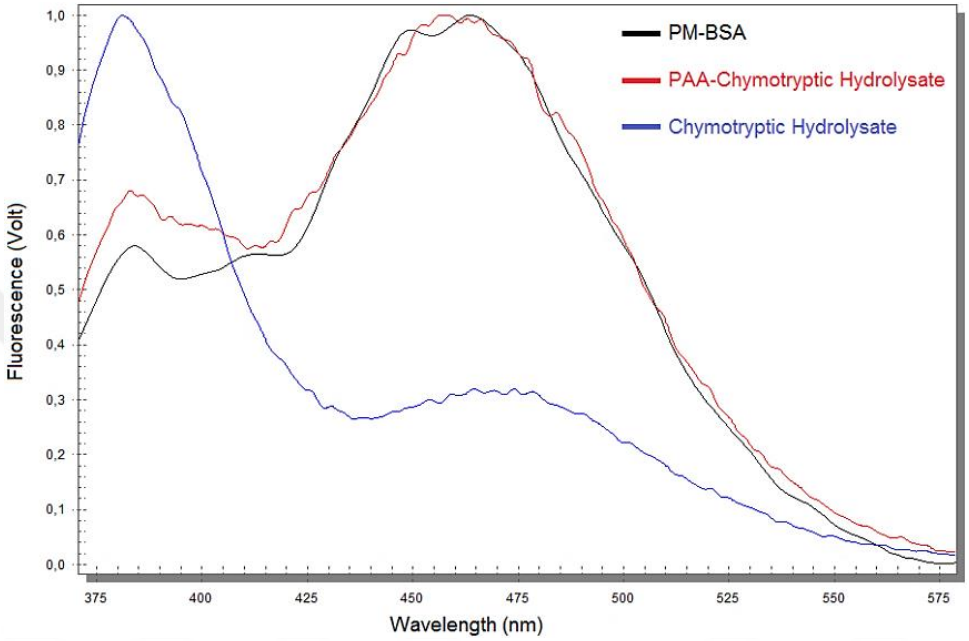

Figure 4.14 Time-resolved fluorescence spectra taken before and after treatment of PM-BSA solution with free chymotrypsin and PAA-chymotrypsin conjugate in Tris.HCl buffer (0.025 M, 0.1 M NaCl, 0.005 M $CaCl_2$, pH: 8)2ml . λ_{exc}: 337 nm ; $\lambda_{emis.max}$:384 nm (monomer); $\lambda_{emis.max}$:464nm (excimer)

When the changes in fluorescence spectra of PM-BSA complex after the hydrolyses with free chymotrypsin and PAA-chymotrypsin were compared (Figure 4.14); as a result, the hydrolysis with free chymotrypsin caused a large amount of decreasing in excimer emission maximum at 464nm and an increase in monomer emission maximum at 384nm. Accordingly, it can be said that a significant amount of the pairs of planar pyrene rings positioned face to face at appropriate distances causing excimer emissions, have lost their positions due to the hydrolytic effect of free chymotrypsin. Hydrolysis of PM-BSA with the PAA-chymotrypsin does not make any significant change except a small increase in monomer emission giving the maximum at 384 nm in the emission spectrum. Accordingly, chymotrypsin significantly lost its activity in the conjugate with PAA and was inhibited. These results support the data obtained from UV-VIS measurements.

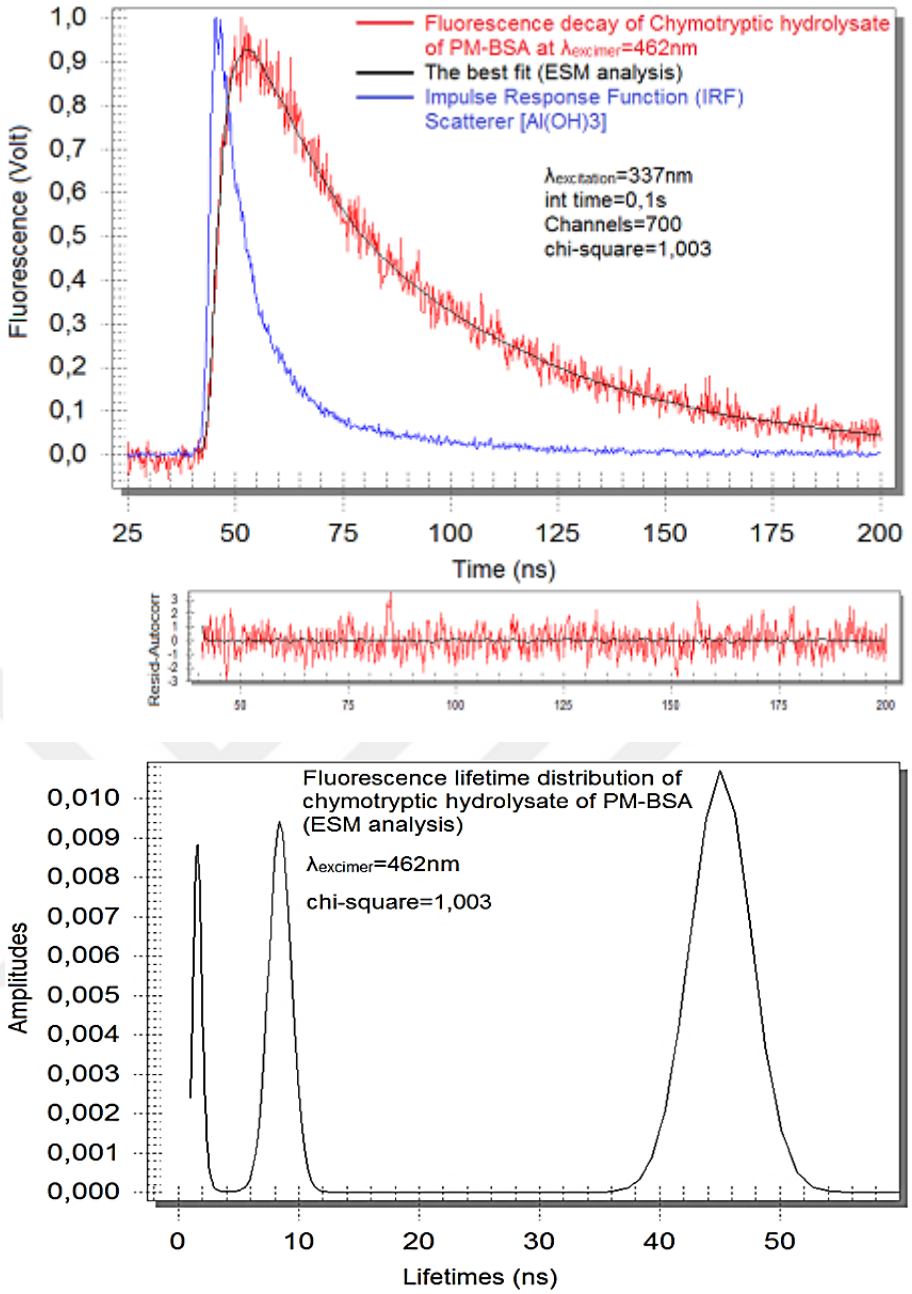

Figure 4.15 Fluorescence decay curve of free chymotrypsin hydrolysate of PM-BSA solution in Tris.HCl buffer (0.025M, 0.1M NaCl, 0.005M $CaCl_2$, pH: 8) 2ml , fitting curve of fluorescence decay data and fluorescence lifetime distribution (ESM, Chi-square: 1,003), λ_{exc}: 337 nm; $\lambda_{excimer.max}$: 462 nm; Integration time : 0,1; Channels: 700; averages: 3.

Figure 4.12 shows the fluorescence lifetime distribution obtained from the ESM analysis of the fluorescence decay data of the PM-BSA complex. Figure 4.15 gives the fluorescence lifetime distribution produced by hydrolysis of PM-BSA by free chymotrypsin and in figure 4.16 the fluorescence lifetime distribution produced by hydrolysis of PM-BSA by PAA-chymotrypsin conjugate. When these three distributions

are compared; The distribution after hydrolysis with free chymotrypsin shifting to the left towards with shorter lifetime emissions with an additional peak, and the hydrolysis with conjugate shows a shift to the right towards longer lifetime emissions. According to this, the bioconjugate PAA-chymotrypsin changed the hydrolytic character of chymotrypsin.

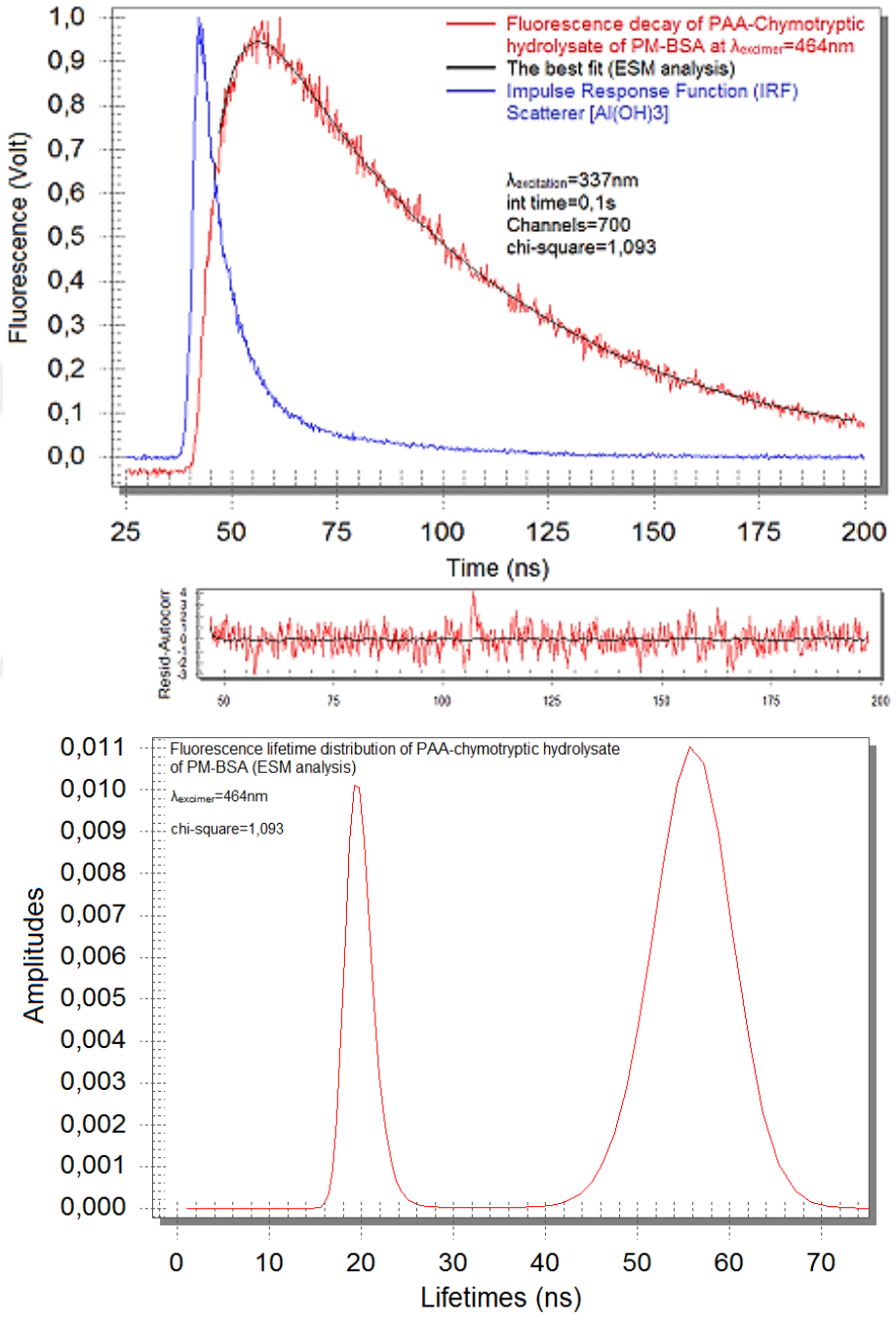

Figure 4.16 Fluorescence decay curve of PAA-chymotrypsin hydrolysate of PM-BSA solution in Tris.HCl buffer (0.025 M, 0.1 M NaCl, 0.005 M $CaCl_2$, pH: 8) 2ml, fitting curve of fluorescence decay data , and fluorescence lifetime distribution (ESM, Chi-square: 1.093). λ_{exc}: 337 nm; $\lambda_{excimer.max}$: 464 nm; Integration time : 0,1; Channels: 700; averages: 3.

The peptide content of hydrolysate obtained by free chymotrypsin is specifically formed by the hydrolytic character of free chymotrypsin. Shorter lifetime distribution of this hydrolysate show that the intereaction of the excimers involved in the structure of the peptide with the solvent molecules increased as expected. Unlike the hydrolysis with free chymotrypsin, the shifting of the distribution towards the right side with the conjugate, indicates that the peptides that hydrolysate have more apolar character and the excimers are stucked in this apolar environment and have less interaction with the solvent molecules and so the hydrolysis was not completed. as a result; it can be said that, PAA-chymotrypsin conjugation using the covalent modification method reduced the activity of chymotrypsin.

CHAPTER 5

RESULTS AND DISCUSSION

The specificity of the hydrolytic effects of proteases makes specific the sizes, shapes, conformations, electrical charges, polarities and chemical environments of the peptides which the proteases produced from a distinct protein, due to the number, variation and sequence differences of the amino acid content of the peptides. Depending on these events, the changes in fluorescence lifetime distributions can take shapes specific to protease activity. Conservation of the activity in polymer-protease conjugates synthesized to increase the stability of the protease is the most important issue.

The changes in fluorescence lifetime distribution of PM-BSA complex in the effect of free chymotrypsin were shown in ref (54).

In this work we examined the modifier effects of covalent conjugate of chymotrypsin with polyacrylic acid (PAA) on fluorescence lifetime distributions of PM-BSA complex by using time resolved spectrofluorometer. The differences between the results of fluorescence spectra (Figure 5.1) and of the fluorescence lifetime distributions (Figure 5.2) obtained from the two proteolytic hydrolysates of PM-BSA produced by the activities of free chymotrypsin and of PAA-conjugated chymotrypsin showed great decreasing in the activity of conjugated chymotrypsin.

In the fluorescence spectrum of free chymotrypsin hydrolysate of PM-BSA complex, the excimer emission maximum at 464 nm was significantly reduced but not consumed, while the monomer emission at 384 nm was significantly increased. This can be explained as the disappearance of the interfacial positions of significant number of the pyrene ring planes forming the excimers by the hydrolysis.

In the fluorescence spectrum of PAA-chymotrypsin conjugate hydrolysate of PM-BSA complex; there is no significant change except for a small increase in monomer

emission at 384nm, indicating a very low amount of hydrolysis and therefore a significant decrease in the activity of chymotrypsin in the bioconjugate. These results support the data obtained from UV-VIS measurements.

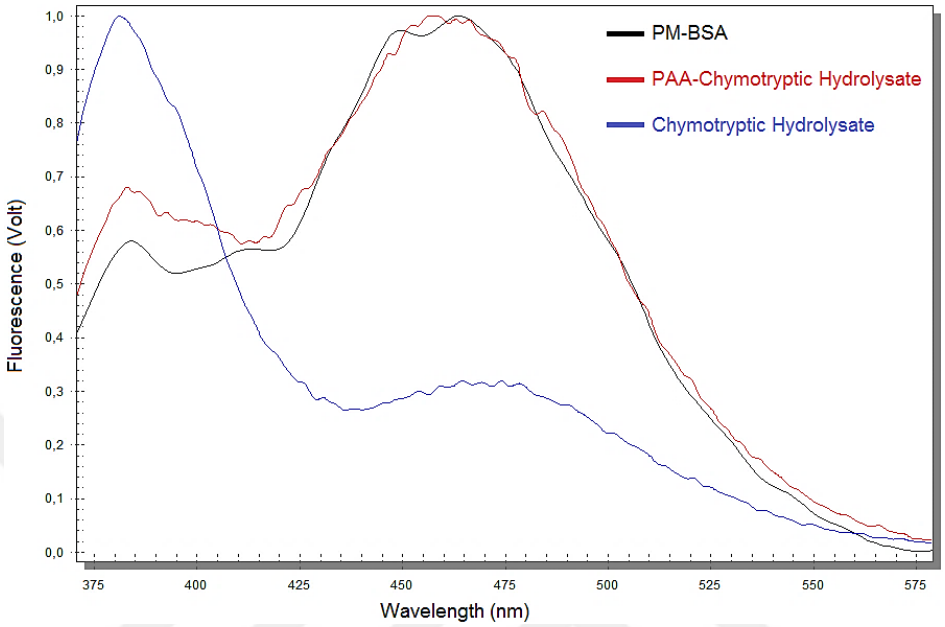

Figure 5.1 Changes of the time-resolved fluorescence spectra of free chymotrypsin and PAA-chymotrypsin conjugate hydrolysates of PM-BSA solution, $\lambda_{excitation} = 337$ nm , $\lambda_{monomer\text{-}max} = 384$ nm, $\lambda_{excimer\text{-}max} = 464$ nm

The differences in fluorescence lifetime distributions are presented comparatively in Figure 5.2. The fluorescence lifetime distribution produced from hydrolysis of PM-BSA complex with free chymotrypsin exhibited a fluorescence character with shorter-lifetime region as expected. The reason of the distribution profile; is that the chemical environments surrounding the excimers after complete hydrolysis have been rearranged to expose more excimers to solvent molecules, relative to pre-hydrolysis conditions.

The fluorescence lifetime distribution produced from hydrolysis of PM-BSA complex with PAA-chymotrypsin conjugate exhibited a shift to the longer-lifetime region (Figure 5.2).

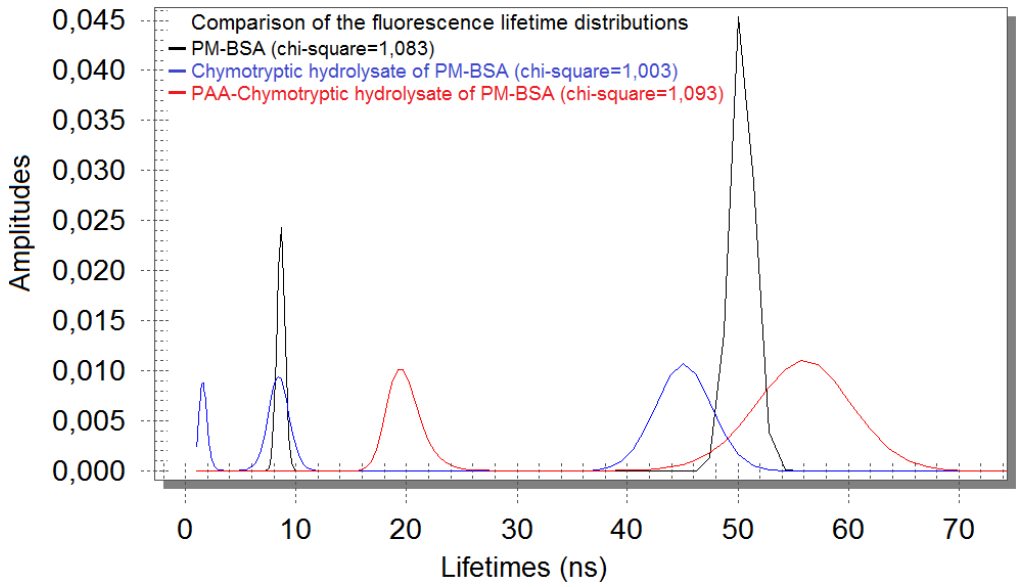

Figure 5.2 Comparison of fluorescence lifetime distributions of free chymotrypsin and PAA-Chymotrypsin hydrolysates of PM-BSA solution , $\lambda_{excitation}$ = 337 nm, $\lambda_{monomer\text{-}max}$ = 384 nm, $\lambda_{excimer\text{-}max}$ = 464 nm, integration time = 0,1s

This is due to the peptides products of incomplete hydrolysis of PM-BSA complex, forming a more protective, or more apolar chemical environment around the excimers against to solvent molecules.

As a result; the conjugation made with polyacrylic acid by using covalent modification method causes a significant decreasing in the activity of chymotrypsin enzyme. This data obtained from the fluorescence lifetime distributions may have importance in determining the methods of conjugation reaction and polymer choosing rightly in bioconjugation researches that will be done with the aim to improve the stability of chymotrypsin-like proteases without losing the activity.

REFERENCES

[1] Hermanson, G.T. (2008). Bioconjugate Techniques, Second Edition, Academic Press, Elsevier Inc., New York.

[2] Lakowicz, J.R. (2006).Principles of Fluorescence Spectroscopy, Third Edition, Springer Science+Business Media, LLC, New York.

[3] Albani, J. R. (2008). Principles and Applications of Fluorescence Spectroscopy. John Wiley and Sons.

[4] Valeur, B. (2002). Molecular Fluorescence, Principles and Applications, WILEY-VCH Verlag GmbH, Weinheim (Federal Republic of Germany).

[5] Hemmilä, I.A. (1991). Applications of Fluorescence in Immunoassays, Chapter 5, John Wıley and Sons, Inc., New York.

[6] Bommarius, A. S., Riebel, B.R. (2004). Biocatalysis, Wiley-VCH Verlag GmbH and Co. KGaA. Weinheim.

[7] Beynon R. ve Bond, J.S. (2001). Proteolytic Enzymes, Second Edition, Oxford University Pres, New York.

[8] Rawlings, N.D., Salvesen, G., (2013). Handbook of Proteolytic Enzymes, 1, Third Edition, Elsevier Ltd., London.

[9] Edwards, D., Høyer-Hansen, G., Blasi, F., Sloane, B. F., (2008). The Cancer Degradome: Proteases and Cancer Biology, Springer Science+Business Media, LLC, New York.

[10] Stubbs, C.D., Williams, B.W., (1992). "Fluorescence in Membranes", Topics in Fluorescence Spectroscopy: Biochemical Applications, 3: 231-271; Editor: Lakowicz, J.R., (1992), Plenum Press, New York.

[11] Barrantes, F.J., Antollini, S.S., Blanton, M.P., Prieto, M., (2000). "Topography of Nicotinic Acetylcholine Receptor Membrane-Embedded Domains", J. Biol. Chem., 275: 37333–37339.

[12] Ahn, T., Kim, J.-S., Choi, H.-I., and Yun, C.-H., (2002). "Development of Peptide Substrates for Trypsin Based on Monomer/Excimer Fluorescence of Pyrene", Analytical Biochemistry, 306: 247–251.

[13] Bains, G., Patel, A.B., Narayanaswami, V., (2011). "Pyrene: A Probe to Study Protein Conformation and Conformational Changes", Molecules, 16: 7909-7935.

[14] Betcher-Lange, S.L., Lehrer, S.S., (1978). "Pyrene Excimer Fluorescence in Rabbit Skeletal αα-tropomyosin Labeled With N-(1-Pyrene)maleimide", J. Biol. Chem., 253: 757-3760.

[15] Wagner, B.D. Ware, W.R. (1990). "Recovery Of Fluorescence Lifetime Distributions: Application To Förster Transfer in Rigid and Viscous Media", J. Phys. Chem., 94: 3489-3494.

[16] Narain, R. (Ed.). (2014). Chemistry of Bioconjugates: Synthesis, Characterization and Biomedical Applications. John Wiley and Sons.

[17] Jung, B., and Theato, P. (2012). Chemical Strategies for the Synthesis of Protein – Polymer Conjugates. In Bio-Synthetic Polymer Conjugates. Springer Berlin Heidelberg, 37-70.

[18] Hermanson, G. T. (2013). Bioconjugate Techniques. Academic Press.

[19] Copeland, R.A. (2000). Enzymes: A Practical Introduction to Structure, Mechanism, and Data Analysis, Second Edition, John Wıley and Sons, Inc. Publication, New York.

[20] Robert, K.M., Granner, D.K., Mayes, P.A.,Rodwell, V.W., (2003). Harper's Illustrated Biochemistry, Twenty-Sixth Edition, McGraw-Hill Companies, United States.

[21] Troop, B. (2011). Molecular Biology, Fourth Edition, Jones and Bartlett Publishers.

[22] Freshet, A. (1999). Structure and Mechanism in Protein Science: A Guide to Enzyme Catalysis and Protein Folding. Macmillan.

[23] https://courses.lumenlearning.com/bio1/chapter/reading-protein-structure/, 12 March 2016

[24] Britt, B.M. (2004). "Understanding Enzyme Structure and Function in Terms of the Shifting Specifity Model", J Biochem Mol Biol, 37: 394-401.

[25] Stryer L, Berg JM, Tymoczko JL. (2002). Biochemistry, Fifth Edition. San Francisco: W.H. Freeman.

[26] Palmer, T., (1991). Understanding Enzymes, Third Edition, Ellis Horwood limited, and Chichester, England.

[27] Prather, K.L.J. (2004) .10.492 - Integrated Chemical Engineering (ICE) Topics: Biocatalysis MIT Chemical Engineering Department, Lecture #1 – Course Overview, Enzyme Classification System.

[28] https://www.rose-hulman.edu/~brandt/Chem330/Enzyme_mech_examples.pdf , 12 March 2016

[29] Harvey, R. A., and Ferrier, D. R. (2011). Biochemistry. Lippincott Williams and Wilkins.

[30] Bisswanger, H., (2008). Enzyme Kinetics, Principles and Methods, Second Edition, WILEY-VCH Verlag GmbH and Co. KGaA, Weinheim.

[31] Leskovac, V., (2004). Comprehensive Enzyme Kinetics, Kluwer Academic Publishers, New York.

[32] Wilson, K., and Walker, J. (Eds.). (2010). Principles and Techniques of Biochemistry and Molecular Biology. Cambridge University Press.

[33] http://depts.washington.edu/cmditr/modules/oled/light_emitting_electrochemical_processes.html, 15 may 2016

[34] Sharma, A., Schulman, S.G. (1999). Introduction to Fluorescence Spectroscopy, John Wiley and Sons, Inc., New York.

[35] Tkachenko, N.V. (2006). Optical Spectroscopy, Methods and Instrumentations, Elsevier Science, Netherlands

[36] Pekcan, O. (1993). ESM Method and Laplace Transform of Klafter-Blumen Equation for DET Analysis in Polymer Blend Like Materials. In MATERIALS RESEARCH SOCIETY SYMPOSIUM PROCEEDINGS, 290: 221. Materials Research Society.

[37] Pekcan, Ö. (1993). "Lifetime Distribution Study on Evolution of Dimensionality in Blend-Like Polymer Films", Chem. Phys. 177: 619-628.

[38] Siemiarczuk, A., Wagner, B.D., Ware, W.R., (1990). "Comparison of the Maximum Entropy and Exponential Series Methods for the Recovery of Distributions of Lifetimes from Fluorescence Lifetime Data", J. Phy. Chem., 94: 1661-1666.

[39] James, D. R., and Ware, W. R. (1986). Recovery of Underlying Distributions of Lifetimes from Fluorescence Decay Data. Chemical Physics Letters, 126(1), 7-11.

[40] James, D. R., Siemiarczuk, A., and Ware, W. R. (1992). Stroboscopic Optical Boxcar Technique for the Determination of Fluorescence Lifetimes. Review of Scientific Instruments, 63(2), 1710-1716.

[41] Pekcan, Ö. (1996). "Fluorescence Lifetime Distributions: Applications to High and Low Viscosity Media in Polymer Blend-Like Particles", Eur. Polym. J., 32: 117-124.

[42] Birks, J.B. (1975). "Excimers", Rep. Prog. Phys., 38: 903-974.

[43] Mahara A., R. Iwase, T. Sakamoto, K. Yamana, T. Yamaoka and A. Murakami, (2002). Bispyrene-Conjugated 2-O-Methyloligonucleotide as a Highly Specific RNA-Recognition Brobe. Angewandte Chem., 114: 3800-3802.

[44] Panda, D., Bhattacharyya, B., (1992). "Excimer Fluorescence of Pyrene-Maleimide-Labeled Tubulin", Eur. J. Biochem., 204: 783-787.

[45] Montalti, M., Credi, A., Prodi, L., Gandolfi, M. T., (2006). Handbook of Photochemistry, Chapter 1, CRC Press, Taylor & Francis Group, New York.

[46] Striegel, A.M., Yau, W. W., Kirkland, J. J., Bly, D. D., (2009). Modern Size-Exclusion Liquid Chromatography – Practice of Gel Permeation and Gel Filtration Chromatography, Second Edition, John Wiley and Sons Inc., Hoboken, New

[47] Dubey, V. K. (2014). Proteomics and Genomics. Lecture 5. Size Exclusion (Gel Filtration) Chromatography.

[48] Hegyi, G., Kardos, J., Kovács, M., Málnási-Csizmadia, A., Nyitray, L., Pál, G., and Venekei, I. (2013). Introduction to Practical Biochemistry. ELTE Faculty of Natural Sciences, Institute of Biology.

[49] Means, G. E. and Feeney, R. E., (1971). Chemical Modification of Proteins, Holden-Day, San Francisco, CA.

[50] Lundblad, R. L., (2004). Chemical Reagents for Protein Modification, Third Edition, CRC Press, Boca Raton, FL, 139.

[51] Wong, S. S., & Jameson, D. M. (2011). Chemistry of Protein and Nucleic Acid Cross-Linking and Conjugation. CRC Press.

[52] Suhr, H., (1964). Effect of the Leaving Group on the Velocity of Nucleophilic Aromatic Substitutions, Berichte, 97, 3268.

[53] http://www.friedli.com/research/PhD/chapter5a.html , 12 Kasım 2014, 22 May 2016

[54] Özyiğit, İ. E., Karakuş, E., & Pekcan, Ö. (2016). The Modifier Effects of Chymotrypsin and Trypsin Enzymes on Fluorescence Lifetime Distribution of "N-(1-pyrenyl) Maleimide–Bovine Serum Albumin" Complex. Spectrochimica Acta Part A: Molecular and Biomolecular Spectroscopy, 154, 8-12.

[55] Marquez, J., Iriarte, A., Martinez-Carrion, M., (1989). "Covalent Modification of a Critical Sulfhydryl Group in the Acetylcholine Receptor: Cysteine-222 of the a-Subunit", Biochemistry, 28: 7433-7439.

[56] Wu, C.-W., Yarbrough, L. R., Wu, F.Y.-H., (1976). "N-(1 -Pyrene)Maleimide: A Fluorescent Cross-Linking Reagent", Biochemistry, 15(13): 2863-2868.

[57] The T.H., Feltkamp T.E.W., (1970). "Conjugation of Fluorescein Isothiocyanate to Antibodies; I. Experiments on The Conditions of Conjugation", Immunology, 18: 865-873.

[58] Karahan, M., Mustafaeva, Z., & Özeroğlu, C. (2010). Investigation of Ternary Complex Formations of Polyacrylic Acid with Bovine Serum Albumin in the Presence of Metal Ions by Fluorescence and Dynamic Light Scattering Measurements. The Brotein Journal, 29(5), 336-342.

[59] Bender, M. L., Kezdy, F. J., and Wedler, F. C. (1967). Alpha-Chymotrypsin: Enzyme Concentration and Kinetics. J. Chem. Educ, 44(2), 84.

CURRICULUM VITAE

PERSONAL INFORMATION

Name and surname : Sama Amer ABBAS

Date of Birth and place : 6-1-1990/Tikrit,Iraq

Foreign language : English

E-mail : smsmamer99@yahoo.com

EDUCATION STATUS

Degree	Department	University	Date of Graduation
Undergraduate	Chemistry	University Of Tikrit	2011
High school	Science	Tikrit Lilmutamayizat High school	2007